Symmetric Clifford twirling for cost-optimal quantum error mitigation in early FTQC regime

Kento Tsubouchi, 1, * Yosuke Mitsuhashi, 2 Kunal Sharma, 3 and Nobuyuki Yoshioka 1, 4, 5, †

¹Department of Applied Physics, University of Tokyo, 7-3-1 Hongo, Bunkyo-ku, Tokyo 113-8656, Japan
²Department of Basic Science, University of Tokyo, 3-8-1 Komaba, Meguro-ku, Tokyo 153-8902, Japan
³IBM Quantum, IBM T.J. Watson Research Center, Yorktown Heights, NY 10598, USA
⁴Theoretical Quantum Physics Laboratory, RIKEN Cluster for Pioneering Research (CPR), Wako-shi, Saitama 351-0198, Japan
⁵JST, PRESTO, 4-1-8 Honcho, Kawaguchi, Saitama, 332-0012, Japan

Twirling noise affecting quantum gates is essential in understanding and controlling errors, but applicable operations to noise are usually restricted by symmetries inherent in quantum gates. In this Letter, we propose symmetric Clifford twirling, a Clifford twirling utilizing only symmetric Clifford operators that commute with certain Pauli subgroups. We fully characterize how each Pauli noise is converted through the twirling and show that certain Pauli noise can be scrambled to a noise exponentially close to the global white noise. We further demonstrate that the effective noise of some highly structured circuits, such as Trotterized Hamiltonian simulation circuits, is scrambled to global white noise, and even a single use of CNOT gate can significantly accelerate the scrambling. These findings enable us to mitigate errors in non-Clifford operations with minimal sampling overhead in the early stages of fault-tolerant quantum computing, where executing non-Clifford operations is expected to be significantly more challenging than Clifford operations. Furthermore, they offer new insights into various fields of physics where randomness and symmetry play crucial roles.

Introduction.— As a powerful countermeasure for errors affecting quantum computers, fault-tolerant quantum computing (FTQC) using quantum error correction has been studied in recent decades [1–8]. In many quantum error-correcting codes, Clifford gates can be executed transversally, preventing the propagation of physical errors within code blocks and simplifying their fault-tolerant implementation. Meanwhile, sophisticated techniques such as magic state distillation and gate teleportation are necessary to perform non-Clifford operations fault-tolerantly, resulting in significant overhead in realizing FTQC [9–15]. Therefore, in the early stages of FTQC, known as the early FTQC regime, we anticipate that non-Clifford operations will be susceptible to a nonnegligible amount of logical errors.

In recent years, it has been revealed that such logical errors can be alleviated using a technique known as quantum error mitigation (QEM) [16–18]. The idea of QEM is to predict the expectation value of an ideal error-free quantum circuit by sampling error-prone quantum circuits multiple times and subsequently classically postprocessing the sampling results [19–22]. While a QEM method called probabilistic error cancellation [19, 23, 24] can effectively mitigate such logical errors [16–18], it is not cost-optimal: there exists a quadratic gap between its sampling cost and the lower bound on the sampling cost [25]. Given that reducing the sampling cost can relax the noise requirements in noisy non-Clifford operations and significantly decrease the hardware overhead, it is imperative to develop a cost-optimal QEM method that saturates the lower bound.

When the noise following non-Clifford operations can be characterized as global white noise (also known as global depolarizing noise), it is known that we can costoptimally mitigate errors by simply rescaling the noisy expectation value [25]. A straightforward approach to converting noise to global white noise is Clifford twirling: by randomly inserting global Clifford operations before and after the noise channel, we can scramble the noise to global white noise [26]. However, since the noise channels cannot be divided from non-Clifford operations, it is in principle not possible to insert additional Clifford operations in between, and thus prohibits the full Clifford twirling. One solution is to utilize only the Clifford operations that commutes with the non-Clifford gates, as is proposed for Pauli twirling in Ref. [27]. However, the method only considers local operation for a single Pauli rotation, and hence does not contribute to accelerate white noise approximation. In order to fully exemplify the early FTQC scheme, it is an urgent task to establish a unified understanding and methodology regarding the full symmetric Clifford operations.

In this Letter, we overcome this issue by proposing symmetric Clifford twirling, a Clifford twirling using symmetric Clifford operators [28] that commute with certain Pauli subgroups. By appropriately choosing the Pauli subgroup, we obtain symmetric Clifford operators that commute also with non-Clifford operations, allowing us to twirl its noise. We completely characterize how Pauli noise channels are converted through symmetric Clifford twirling and show that some Pauli noise can be scrambled to the noise exponentially close to the global white noise, enabling the cost-optimal QEM. Moreover, we show that the effective noise channel of some highly structured circuits is scrambled to global white noise (which is called the white-noise approximation [29]), and we can accelerate the scrambling only by a single use of

^{*} tsubouchi@noneq.t.u-tokyo.ac.jp

[†] nyoshioka@ap.t.u-tokyo.ac.jp

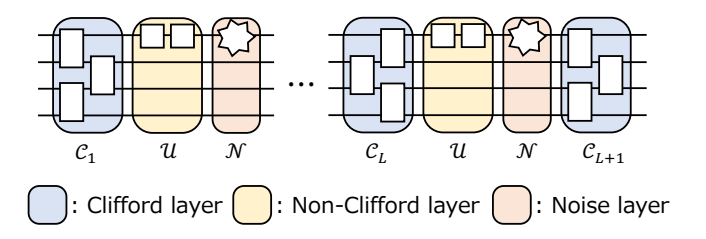


FIG. 1. Quantum circuit structure for the early FTQC regime. This logical circuit consists of three types of layers: a noiseless Clifford operation layer C_l , a non-Clifford operation layer \mathcal{U} , and a subsequent layer of noise channel \mathcal{N} .

CNOT gate. We apply our techniques to the Trotterized Hamiltonian simulation of spin models and validate the efficacy of both symmetric Clifford twirling and the white-noise approximation in the early FTQC era.

Problem setup.— Let us start by introducing a logical quantum circuit structure that encapsulates the essence of the early FTQC regime, as depicted in Fig. 1. This nqubit logical circuit comprises L sequences of the following three layers: a noiseless layer C_l consisting of Clifford operations, a layer \mathcal{U} featuring non-Clifford operations, and a subsequent layer of noise channel \mathcal{N} , where the subscript l is an index to identify each layer and we assume for simplicity that the non-Clifford layer $\mathcal U$ and the noise layer \mathcal{N} are identical for all layers. While the Clifford layer C_l may also be subject to a small amount of logical error, it is expected that logical error is dominated by the non-Clifford layer \mathcal{U} , since we cannot supply a large number of logical qubits for magic state factory in the early FTQC era and hence we shall choose magic state distillation procotol with mild suppression and low space overhead [30, 31]. Therefore, we assume that errors of Clifford layers can be neglected for simplicity (see Sec. S1 of Supplementary Materials (SM) [32] for details).

The non-Clifford layer \mathcal{U} involves various non-Clifford gates such as the T gate, the Toffoli gate, and (synthesized) Pauli rotation gates. Consequently, the noise layer \mathcal{N} can arise from a noisy magic state (in the case of the T gate or the Toffoli gate) or coherent errors caused by the lack of T gates (in the case of Pauli rotation gates). Such noise tends to be Pauli noise, since the noise affecting non-Clifford gates belonging to the third level of the Clifford hierarchy [33], such as the T gate or the Toffoli gate, can be Pauli twirled to be Pauli noise [21], and algorithmic error affecting synthesized non-Clifford gate can be transformed into Pauli noise using randomized compiling [34]. Therefore, we assume that the noise layer is Pauli noise $\mathcal{N} := (1 - p_{\text{err}})\mathcal{I} + \sum_i p_i \mathcal{E}_{P_i}$, where Pauli error $\mathcal{E}_{P_i}(\cdot) := P_i \cdot P_i$ occurs with probability p_i with $p_{\text{err}} := \sum_i p_i$ being the error probability.

While the accumulation of the noise \mathcal{N} can ruin the logical quantum state, we can still estimate the expectation value of some observable by employing QEM techniques. A significant drawback of QEM is that the sampling overhead—a multiplicative factor in the number of

circuit executions needed to restore the ideal expectation value—increases exponentially with the number of noisy layers L [25, 35, 36]. However, if the error probability $p_{\rm err}$ remains sufficiently low, and the total error rate $p_{\rm tot} := p_{\rm err} L$ can be treated as constant, we can mitigate errors with a constant sampling overhead. In the early FTQC regime, we expect the error probability $p_{\rm err}$ to be smaller than the noisy intermediate-scale quantum (NISQ) regime, and we may implement deeper quantum circuit as L = O(poly(n)) with small sampling overhead.

Particularly when we can transform the noise layer \mathcal{N} into global white noise, defined as

$$\mathcal{N}_{\text{wn}, p_{\text{err}}} := (1 - p_{\text{err}})\mathcal{I} + p_{\text{err}} \mathbb{E}_i [\mathcal{E}_{P_i}], \tag{1}$$

where \mathbb{E}_i represents the uniform average over all Pauli noises P_i , we can mitigate errors with a constant sampling overhead of $e^{2p_{\text{tot}}}$ by just rescaling the noisy expectation value. This sampling overhead is not only quadratically improved from that of the previous work using probabilistic error cancellation, which scales as $e^{4p_{\text{tot}}}$ [16–18], but also achieves the theoretical lower bound on the sampling overhead of QEM [25] (see Sec. S2 of SM [32] for details). Therefore, in this Letter, we aim to convert the noise layer \mathcal{N} into the global white noise $\mathcal{N}_{\text{wn},p_{\text{err}}}$ for cost-optimal QEM.

Symmetric Clifford twirling.— One naive way to achieve this goal is to perform Clifford twirling: by applying random Clifford unitary $D \in \mathcal{G}_n$ and its conjugation D^{\dagger} before and after the noise layer \mathcal{N} , where \mathcal{G}_n represents the n-qubit Clifford group, we can scramble the noise layer \mathcal{N} into the global white noise $\mathcal{N}_{\text{Wn},p_{\text{err}}}$ as

$$\mathscr{T}(\mathcal{N}) := \mathbb{E}_{D \in \mathcal{G}_n}[\mathcal{D}^{\dagger} \circ \mathcal{N} \circ \mathcal{D}] = \mathcal{N}_{\mathrm{wn}, p_{\mathrm{err}}}, \qquad (2)$$

where $\mathcal{D}(\cdot) := D \cdot D^{\dagger}$ and \mathscr{T} denotes the superchannel representing Clifford twirling [26]. This operation is, however, not considered as a practical option in the community, since the noise is inseparable from the target non-Clifford unitary. In order to insert D before the noise layer \mathcal{N} , one must insert $U^{\dagger}DU$ before the non-Clifford layer \mathcal{U} , which may introduce additional errors if $U^{\dagger}DU$ is a non-Clifford unitary. One feasible alternative is to consider Clifford unitaries D that commute with U, since $U^{\dagger}DU = D$ becomes a Clifford unitary in this case. This allows us to perform the twirling with negligible errors.

To characterize Clifford unitaries that commute with U, let us denote the set of n-qubit Pauli operator as $\mathcal{P}_n := \{I, X, Y, Z\}^{\otimes n}$ and define a Pauli subgroup

$$Q_U := \langle \{ P \in \mathcal{P}_n \mid \text{tr}[PU] \neq 0 \} \rangle, \tag{3}$$

where $\langle \cdot \rangle$ represents the group generated by the elements within the brackets. Additionally, let us define the Q_{U} -symmetric Clifford group as:

$$\mathcal{G}_{n,\mathcal{Q}_U} := \{ C \in \mathcal{G}_n \mid \forall P \in \mathcal{Q}_U, \ [C,P] = 0 \}, \tag{4}$$

where its complete and unique construction method using simple quantum gates is given in Ref. [28]. From the

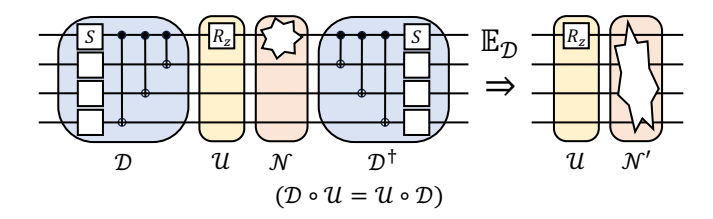


FIG. 2. Conceptual diagram of symmetric Clifford twirling. By randomly sampling Clifford unitary $\mathcal{D} = D \cdot D^{\dagger}$ that commutes with non-Clifford layer $\mathcal{U} = U \cdot U^{\dagger}$, we can scramble the noise layer \mathcal{N} without affecting \mathcal{U} .

definition, $D \in \mathcal{G}_{n,\mathcal{Q}_U}$ commutes with the non-Clifford operator U, enabling us to twirl the noise layer \mathcal{N} using symmetric Clifford unitary $D \in \mathcal{G}_{n,\mathcal{Q}_U}$. We term this twirling as symmetric Clifford twirling, whose effect is represented using a superchannel defined as:

$$\mathscr{T}_{Q_U}(\mathcal{N}) := \mathbb{E}_{D \in \mathcal{G}_{n,\mathcal{Q}_U}}[\mathcal{D}^{\dagger} \circ \mathcal{N} \circ \mathcal{D}]. \tag{5}$$

For the sake of clarity, let us first consider the scenario where the non-Clifford layer \mathcal{U} consists of either the T gate or the Pauli-Z rotation gate $R_z(\theta)$ applied to the first qubit, and the noise layer \mathcal{N} introduces Pauli noise affecting solely the first qubit. In this particular case, \mathcal{Q}_U simplifies to $\mathcal{Q}_U = \{I, Z\} \otimes \{I\}^{\otimes n-1}$, and we can express the effect of symmetric Clifford twirling to the Pauli noise as presented in the following proposition.

Theorem 1 (special case). Let $\mathcal{E}_{P\otimes\mathbb{I}^{\otimes n-1}}(\cdot) = (P\otimes\mathbb{I}^{\otimes n-1}) \cdot (P\otimes\mathbb{I}^{\otimes n-1})$ be a single-qubit Pauli channel with P = X, Y, Z and $\mathcal{Q}_U = \{I, Z\} \otimes \{I\}^{\otimes n-1}$. Then, by applying symmetric Clifford twirling to the Pauli channel as $\mathcal{T}_{\mathcal{Q}_U}(\mathcal{E}_{P\otimes\mathbb{I}^{\otimes n-1}}) = \mathbb{E}_{D\in\mathcal{G}_{n,\mathcal{Q}_U}}[\mathcal{D}^{\dagger} \circ \mathcal{E}_{P\otimes\mathbb{I}^{\otimes n-1}} \circ \mathcal{D}]$, we can scramble the Pauli-X and Y channels as

$$\mathscr{T}_{Q_U}(\mathcal{E}_{P\otimes \mathbf{I}^{\otimes n-1}}) = \underset{\substack{Q_1 \in \{\mathbf{X}, \mathbf{Y}\}\\Q_2 \in \mathcal{P}_{n-1}}}{\mathbb{E}} [\mathcal{E}_{Q_1 \otimes Q_2}] \tag{6}$$

for P = X, Y, while the Pauli-Z channel cannot be scrambled through the symmetric Clifford twirling:

$$\mathcal{T}_{\mathcal{Q}_{II}}(\mathcal{E}_{\mathbf{Z}\otimes\mathbf{I}^{\otimes n-1}}) = \mathcal{E}_{\mathbf{Z}\otimes\mathbf{I}^{\otimes n-1}}.$$
 (7)

Theorem 1 indicates that Pauli-Z noise remains unscrambled, while Pauli-X and Y noise are well dispersed among other qubits (albeit not entirely to global white noise) through symmetric Clifford twirling, and becomes exponentially close to global white noise (Table I). This encourages us to devise a method for implementing the T gate or the $R_z(\theta)$ gate such that the predominant error is Pauli-X or Y error [34]. Alternatively, we may focus on mitigating Pauli-Z noize using probabilistic error cancellation and subsequently use symmetric Clifford twirling to address the remaining Pauli-X and Y noise.

It is worth noting that n-qubit Clifford unitary $D \in \mathcal{G}_{n,\mathcal{Q}_U}$ can be implemented with negligible errors using multi-qubit Pauli measurement (see Sec. S1 of SM [32]

TABLE I. Reduction rate in the distance between the Pauli noise affecting the first qubit with error probability p_{err} and global white noise $\mathcal{N}_{\text{wn},p_{\text{err}}}$ before and after symmetric Clifford twirling. The distance metric we use is the 2-norm v of the error probabilities p_i we define in SM, which can be used to bound the bias between the ideal and mitigated expectation value (see Sec. S3 of SM [32] for details).

Noise model	Pauli Z	depolarizing	Pauli X or Y
$\overline{\text{Reduction rate of } v}$	1	$1/\sqrt{3}$	2^{-n}

for details). Furthermore, even if the implementation of n-qubit Clifford unitary results in a non-negligible amount of logical errors, we can still effectively scramble the noise to some extent by limiting the sampled symmetric Clifford unitary to 2-qubit Clifford unitaries that always acts nontrivially on the first qubit. We call such a twirling 2-sparse symmetric Clifford twirling, where we can scramble Pauli-X and Y noise to a uniform distribution of Pauli noise with 2-qubit Pauli noise, and obtain a noise that is polynomially close to the global white noise. We note that this process can be performed using only a single CNOT gate and some single-qubit Clifford gates, allowing us to scramble noise with minimal additional errors. We may also generalize such a sparse twirling to involve k-local Clifford gates to complete the symmetric Clifford twirling up to the kth order (see Sec. S4 of SM [32] for details).

Now, let us generalize Theorem 1 to arbitrary non-Clifford unitary U, so that we can apply symmetric Clifford twirling to any non-Clifford gates such as the Toffoli gate or multi-qubit Pauli rotation gates. In Ref. [28], it was shown that arbitrary Pauli subgroup \mathcal{Q}_U can be decomposed into three parts as

$$Q_{IJ} = W^{\dagger}(\{\mathbf{I}, \mathbf{X}, \mathbf{Y}, \mathbf{Z}\}^{\otimes n_1} \otimes \{\mathbf{I}, \mathbf{Z}\}^{\otimes n_2} \otimes \{\mathbf{I}\}^{\otimes n_3})W \quad (8)$$

up to phase, using a Q_U -dependent Clifford unitary $W \in \mathcal{G}_n$ and $n_1 + n_2 + n_3 = n$. By using the decomposition in Eq. (8), we obtain the following theorem.

Theorem 2 (general case). Let $P \in \mathcal{P}_n$ be an n-qubit Pauli operator, $\mathcal{E}_P(\cdot) = P \cdot P$ be the corresponding Pauli channel, and \mathcal{Q}_U be a Pauli subgroup defined as in Eq. (3). Let us decompose \mathcal{Q}_U as in Eq. (8) and represent P as $P = W^{\dagger}(P_1 \otimes P_2 \otimes P_3)W$ up to phase, where $P_1 \in \mathcal{P}_{n_1}$, $P_2 \in \mathcal{P}_{n_2}$, and $P_3 \in \mathcal{P}_{n_3}$. Then, the Pauli channel scrambled through symmetric Clifford twirling $\mathcal{T}_{\mathcal{Q}_U}(\mathcal{E}_P) = \mathbb{E}_{D \in \mathcal{G}_{n,\mathcal{Q}_U}}[\mathcal{D}^{\dagger} \circ \mathcal{E}_P \circ \mathcal{D}]$ can be represented as:

(i) when
$$P_2 \notin \{I, Z\}^{\otimes n_2}$$
,

$$\mathscr{T}_{\mathcal{Q}_U}(\mathcal{E}_P) = \underset{\substack{Q_2 \in \{I, Z\}^{\otimes n_2} \\ Q_3 \in \mathcal{P}_{n_3}}}{\mathbb{E}} \left[\mathcal{E}_{W^{\dagger}(P_1 \otimes P_2 Q_2 \otimes Q_3)W} \right], \quad (9)$$

(ii) when
$$P_2 \in \{\mathbf{I}, \mathbf{Z}\}^{\otimes n_2}$$
 and $P_3 \neq \mathbf{I}^{\otimes n_3}$,
$$\mathcal{T}_{\mathcal{Q}_U}(\mathcal{E}_P) = \underset{\substack{Q_2 \in \{\mathbf{I}, \mathbf{Z}\}^{\otimes n_2} \\ Q_3 \in \mathcal{P}_{n_3} \setminus \{\mathbf{I}\}^{\otimes n_3}}}{\mathbb{E}} \left[\mathcal{E}_{W^{\dagger}(P_1 \otimes Q_2 \otimes Q_3)W} \right], \quad (10)$$

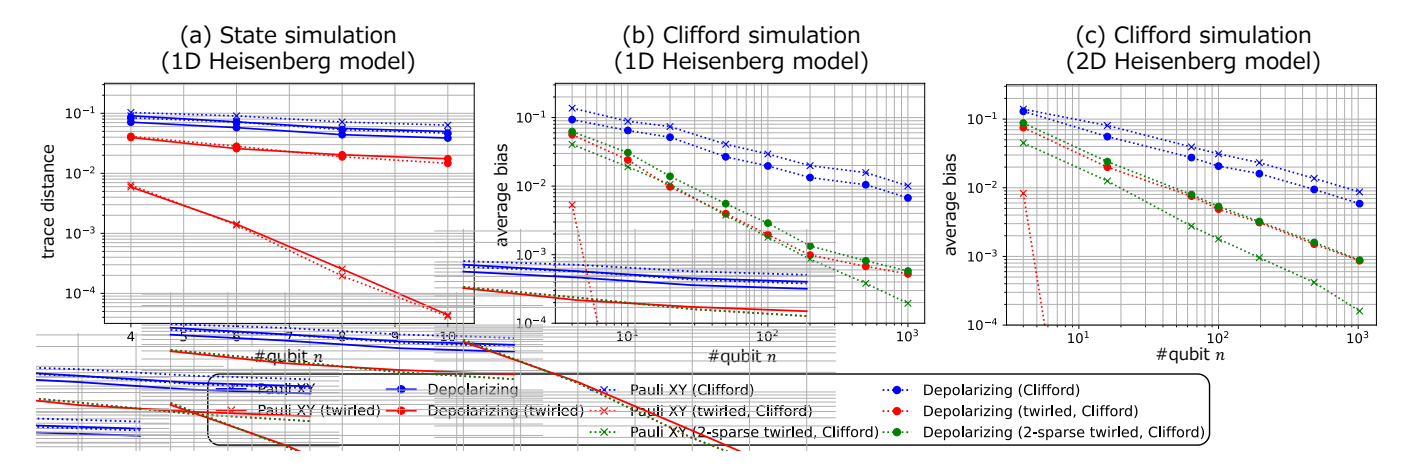


FIG. 3. Qubit count dependence of the performance of symmetric Clifford twirling for Trotterized Hamiltonian simulation of (a) and (b): 1D and (c): 2D Heisenberg model. Panel (a) represents the trace distance between the ideal noiseless state ρ_{ideal} and the rescaled virtual noisy state $R\rho_{\text{noisy}} + (1-R)I/2^n$, where the rescaling coefficient R is defined in Sec. S6 of SM [32]. Panel (b) and (c) represents the average bias over random Pauli operators $P \in \mathcal{P}_n$ defined as $|R2^{-n}|\text{tr}[\mathcal{N}_{\text{eff}}(P)P]| - 1|$, where $\mathcal{N}_{\text{eff}} = \mathcal{C}_{L+1} \circ \mathcal{N} \circ \mathcal{U} \circ \cdots \circ \mathcal{C}_1 \circ \mathcal{C}_1^{-1} \circ \cdots \circ \mathcal{U}^{-1} \circ \mathcal{C}_{L+1}^{-1}$ is the effective noise channel. We fix the total error rate as $p_{\text{tot}} := p_{\text{err}}L = 1$ and set the Trotter step size as 100 for (a) and (b) and 50 for (c). The circle and the x dots represent the result for depolarizing noise and Pauli X noise, while the red, blue, and green lines represent the results without symmetric Clifford twirling, with symmetric Clifford twirling, and with 2-sparse twirling. The dotted line represents the result of the Clifford circuit, where $U = R_z(\theta)$ gate is replaced with $R_z(\pi/2) = S$ gate.

(iii) when
$$P_2 \in \{I, Z\}^{\otimes n_2}$$
 and $P_3 = I^{\otimes n_3}$,
 $\mathscr{T}_{\mathcal{Q}_U}(\mathcal{E}_P) = \mathcal{E}_P$. (11)

By using Theorem 2, we can discuss how the noise affecting general non-Clifford unitary such as the Toffoli gate or multi-qubit Pauli rotation gates can be scrambled through symmetric Clifford twirling. We provide the proof of Theorem 2 in Sec. S7 of SM [32]. We note that Theorem 1 directly follows from Theorem 2 by setting W=I and $n_1=0, n_2=1, n_3=n-1$.

Numerical analysis. — To evaluate the efficacy of symmetric Clifford twirling in mitigating errors, we apply our techniques to the dynamics simulation circuit of first-order Suzuki-Trotter decomposition for the 1D and 2D Heisenberg models with the open boundary condition. In this setup, we assume that the non-Clifford layer \mathcal{U} is the $R_z(\theta)$ gate acting on the first qubit, which is transformed into a 2-qubit Pauli rotation gate by the Clifford layer to execute each Trotter step. As for the noise layer, we assume that \mathcal{N} represents either Pauli noise consisting of Pauli-X and Y errors with equal probabilities or depolarizing noise acting on the first qubit. We set the total error rate to $p_{\text{tot}} = 1$, which results in the constant sampling overhead of $e^2 \sim 7$.

Fig. 3 (a) represents the trace distance between the ideal noiseless state ρ_{ideal} and the rescaled virtual noisy state $R\rho_{\text{noisy}} + (1-R)I/2^n$ for the 1D Heisenberg model, where the optimal rescaling coefficient R is defined in Sec. S6 of SM [32]. We note that the trace distance upper bounds the bias in mitigating errors. We observe that the trace distance for symmetric Clifford-twirled Pauli-X and Y noise converges exponentially to 0, corroborating

the result in Theorem 1 which states that Pauli-X and Y noise can be twirled into a noise that is exponentially close to the global white noise, while scrambling of Pauli-Z noise is prohibited. This result motivates us to devise a method for synthesizing the $R_z(\theta)$ gate with the dominant algorithmic error being Pauli-X or Y noise. Such a gate compilation is achieved in a probabilistic way under some scenarios [34], while it is an open question what control one can have to transform the noise in such cases.

To demonstrate the effectiveness of symmetric Clifford twirling in large-scale quantum circuits, where the quantum advantage is expected, we perform a largescale Clifford simulation by replacing the $R_z(\theta)$ gate with $R_z(\pi/2) = S$ gate in Fig. 3 (b) and (c). Here, we observe that bias between ideal and error-mitigated expectation value decreases roughly as $1/\sqrt{n}$ as we increase the aubit count, even without performing symmetric Clifford twirling. This can be considered as the effect of white-noise approximation [29], where the effective noise of the quantum circuit is scrambled to the global white noise. We can view the symmetric Clifford twirling as a method to accelerate the noise scrambling in whitenoise approximation, which holds true even for depolarizing noise where Pauli-Z noise exists. Furthermore, we can still accelerate the noise scrambling by only sparsely twirling the noise using a 2-qubit symmetric Clifford operator, and improve the scaling of the bias from $1/\sqrt{n}$ to 1/n when there is no Pauli-Z noise. We emphasize that the difference in the performance of the full twirling and the sparse twirling is negligible when the Pauli-Z noise remains untwirled, as we can see from the results of depolarizing noise.

Given the similarity of results between Clifford and non-Clifford state simulations in Fig. 3 (a), we can anticipate that the same principle also applies to large-scale non-Clifford quantum circuits achieving a quantum advantage. It is worth noting that the validity of the white-noise approximation for such highly structured circuits is a phenomenon unique to the early FTQC regime. In fact, it is known that the approximation fails for shallow, log-depth quantum circuits in the NISQ regime [37]. We further discuss the white-noise approximation in the early FTQC regime in Sec. S6 of SM [32].

Conclusion.— In this Letter, we have introduced a cost-optimal QEM method aimed at mitigating logical errors in non-Clifford operations with minimal sampling overhead. Our approach centers on the conversion of noise into noise resembling global white noise through symmetric Clifford twirling. We characterize the transformation of Pauli channels under symmetric Clifford twirling and demonstrate its efficacy through numerical simulations in various scenarios. Additionally, we show that deep logical circuits, even the highly structured one, can also help the conversion to global white noise.

We envision a wide variety of future directions. Here we mention the most important two in order. The first is to develop a way to perform non-Clifford unitary with a noise that can be scrambled through symmetric Clifford twirling. For example, the common noise model of T gates executed via gate teleportation is known to be Pauli-Z noise [16, 17], which cannot be twirled. The development of a novel approach to perform T gates with Pauli X or Y errors in the early FTQC regime represents a crucial avenue for future research.

The second is to develop a further application of symmetric Clifford twirling. While our focus in this Letter has been on using symmetric Clifford twirling for cost-optimal QEM, conventional Clifford twirling is also employed in various contexts ranging from fidelity estimation [26, 38] to the analysis of information loss in black holes [39]. Investigating the practical utility of symmetric Clifford twirling for such important tasks in quantum information theory, high energy physics, and many-body physics is left as an interesting future work.

Acknowledgements.— The authors wish to thank Gregory Boyd, Anthony Chen, Suguru Endo, Soumik Ghosh, Christophe Piveteau, Yihui Quek, Takahiro Sagawa, Yasunari Suzuki, Kristan Temme, and Ewout van den Berg for fruitful discussions. K.T. and Y.M. are supported by World-leading Innovative Graduate Study Program for Materials Research, Information, and Technology (MERIT-WINGS) of the University of Tokyo. K.T. is also supported by JSPS KAKENHI Grant No. JP24KJ0857. Y.M. is also supported by JSPS KAKENHI Grant No. JP23KJ0421. N.Y. wishes to thank JST PRESTO No. JPMJPR2119, JST Grant Number JPMJPF2221, JST CREST Grant Number JPMJCR23I4,IBM Quantum, and JST ERATO Grant Number JPMJER2302, Japan.

- [1] P. W. Shor, Scheme for reducing decoherence in quantum computer memory, Physical review A **52**, R2493 (1995).
- [2] E. Knill, R. Laflamme, and W. Zurek, Threshold accuracy for quantum computation, arXiv preprint quantph/9610011 (1996).
- [3] D. Aharonov and M. Ben-Or, Fault-tolerant quantum computation with constant error, in *Proceedings of the twenty-ninth annual ACM symposium on Theory of computing* (1997) pp. 176–188.
- [4] D. A. Lidar and T. A. Brun, Quantum error correction (Cambridge university press, 2013).
- [5] N. Ofek, A. Petrenko, R. Heeres, P. Reinhold, Z. Leghtas, B. Vlastakis, Y. Liu, L. Frunzio, S. Girvin, L. Jiang, et al., Extending the lifetime of a quantum bit with error correction in superconducting circuits, Nature 536, 441 (2016).
- [6] S. Krinner, N. Lacroix, A. Remm, A. Di Paolo, E. Genois, C. Leroux, C. Hellings, S. Lazar, F. Swiadek, J. Herrmann, et al., Realizing repeated quantum error correction in a distance-three surface code, Nature 605, 669 (2022).
- [7] G. Q. AI, Suppressing quantum errors by scaling a surface code logical qubit, Nature 614, 676 (2023).
- [8] D. Bluvstein, S. J. Evered, A. A. Geim, S. H. Li, H. Zhou, T. Manovitz, S. Ebadi, M. Cain, M. Kalinowski, D. Hangleiter, et al., Logical quantum processor based on reconfigurable atom arrays, Nature 626, 58 (2024).
- [9] B. Eastin and E. Knill, Restrictions on transversal en-

- coded quantum gate sets, Physical review letters **102**, 110502 (2009).
- [10] S. Bravyi and A. Kitaev, Universal quantum computation with ideal clifford gates and noisy ancillas, Phys. Rev. A 71, 022316 (2005).
- [11] S. Bravyi and J. Haah, Magic-state distillation with low overhead, Physical Review A 86, 052329 (2012).
- [12] A. G. Fowler, S. J. Devitt, and C. Jones, Surface code implementation of block code state distillation, Scientific reports 3, 1939 (2013).
- [13] A. M. Meier, B. Eastin, and E. Knill, Magic-state distillation with the four-qubit code, arXiv preprint arXiv:1204.4221 (2012).
- [14] D. Litinski, Magic state distillation: Not as costly as you think, Quantum 3, 205 (2019).
- [15] J. O'Gorman and E. T. Campbell, Quantum computation with realistic magic-state factories, Physical Review A 95, 032338 (2017).
- [16] C. Piveteau, D. Sutter, S. Bravyi, J. M. Gambetta, and K. Temme, Error mitigation for universal gates on encoded qubits, Physical review letters 127, 200505 (2021).
- [17] M. Lostaglio and A. Ciani, Error mitigation and quantum-assisted simulation in the error corrected regime, Physical review letters 127, 200506 (2021).
- [18] Y. Suzuki, S. Endo, K. Fujii, and Y. Tokunaga, Quantum error mitigation as a universal error reduction technique: Applications from the nisq to the fault-tolerant quantum computing eras, PRX Quantum 3, 010345 (2022).

- [19] K. Temme, S. Bravyi, and J. M. Gambetta, Error mitigation for short-depth quantum circuits, Physical review letters 119, 180509 (2017).
- [20] S. Endo, Z. Cai, S. C. Benjamin, and X. Yuan, Hybrid quantum-classical algorithms and quantum error mitigation, Journal of the Physical Society of Japan 90, 032001 (2021).
- [21] Z. Cai, R. Babbush, S. C. Benjamin, S. Endo, W. J. Huggins, Y. Li, J. R. McClean, and T. E. O'Brien, Quantum error mitigation, arXiv preprint arXiv:2210.00921 (2022).
- [22] Y. Kim, A. Eddins, S. Anand, K. X. Wei, E. Van Den Berg, S. Rosenblatt, H. Nayfeh, Y. Wu, M. Zaletel, K. Temme, et al., Evidence for the utility of quantum computing before fault tolerance, Nature 618, 500 (2023).
- [23] S. Endo, S. C. Benjamin, and Y. Li, Practical quantum error mitigation for near-future applications, Physical Review X 8, 031027 (2018).
- [24] E. Van Den Berg, Z. K. Minev, A. Kandala, and K. Temme, Probabilistic error cancellation with sparse pauli-lindblad models on noisy quantum processors, Nature Physics, 1 (2023).
- [25] K. Tsubouchi, T. Sagawa, and N. Yoshioka, Universal cost bound of quantum error mitigation based on quantum estimation theory, Physical Review Letters 131, 210601 (2023).
- [26] J. Emerson, R. Alicki, and K. Życzkowski, Scalable noise estimation with random unitary operators, Journal of Optics B: Quantum and Semiclassical Optics 7, S347 (2005).
- [27] Y. Kim, C. J. Wood, T. J. Yoder, S. T. Merkel, J. M. Gambetta, K. Temme, and A. Kandala, Scalable error mitigation for noisy quantum circuits produces competitive expectation values, Nature Physics 19, 752 (2023).
- [28] Y. Mitsuhashi and N. Yoshioka, Clifford group and unitary designs under symmetry, PRX Quantum 4, 040331 (2023).
- [29] A. M. Dalzell, N. Hunter-Jones, and F. G. Brandão, Random quantum circuits transform local noise into global white noise, arXiv preprint arXiv:2111.14907 (2021).
- [30] M. Vasmer and A. Kubica, Morphing quantum codes, PRX Quantum 3, 030319 (2022).
- [31] T. Itogawa, Y. Takada, Y. Hirano, and K. Fujii, Even more efficient magic state distillation by zero-level distillation, arXiv preprint arXiv:2403.03991 (2024).
- [32] See Supplementary Materials for more details (URL to be added).
- [33] D. Gottesman and I. L. Chuang, Quantum teleportation is a universal computational primitive, arXiv preprint quant-ph/9908010 (1999).
- [34] N. Yoshioka, S. Akibue, H. Morisaki, K. Tsubouchi, and Y. Suzuki, Error crafting in probabilistic quantum gate

- synthesis, in preparation (2024).
- [35] R. Takagi, H. Tajima, and M. Gu, Universal sampling lower bounds for quantum error mitigation, Physical Review Letters 131, 210602 (2023).
- [36] Y. Quek, D. S. França, S. Khatri, J. J. Meyer, and J. Eisert, Exponentially tighter bounds on limitations of quantum error mitigation, arXiv preprint arXiv:2210.11505 (2022).
- [37] J. Foldager and B. Koczor, Can shallow quantum circuits scramble local noise into global white noise?, arXiv preprint arXiv:2302.00881 (2023).
- [38] C. Dankert, R. Cleve, J. Emerson, and E. Livine, Exact and approximate unitary 2-designs and their application to fidelity estimation, Physical Review A 80, 012304 (2009).
- [39] P. Hayden and J. Preskill, Black holes as mirrors: quantum information in random subsystems, Journal of high energy physics 2007, 120 (2007).
- [40] D. Litinski, A game of surface codes: Large-scale quantum computing with lattice surgery, Quantum 3, 128 (2019).
- [41] J. Lee, D. W. Berry, C. Gidney, W. J. Huggins, J. R. Mc-Clean, N. Wiebe, and R. Babbush, Even more efficient quantum computations of chemistry through tensor hypercontraction, PRX Quantum 2, 030305 (2021).
- [42] N. Yoshioka, T. Okubo, Y. Suzuki, Y. Koizumi, and W. Mizukami, Hunting for quantum-classical crossover in condensed matter problems, npj Quantum Information 10, 45 (2024).
- [43] M. B. Hastings, Turning gate synthesis errors into incoherent errors, arXiv preprint arXiv:1612.01011 (2016).
- [44] E. Campbell, Shorter gate sequences for quantum computing by mixing unitaries, Phys. Rev. A 95, 042306 (2017).
- [45] E. Magesan, J. M. Gambetta, and J. Emerson, Characterizing quantum gates via randomized benchmarking, Physical Review A 85, 042311 (2012).
- [46] D. Maslov and W. Yang, Cnot circuits need little help to implement arbitrary hadamard-free clifford transformations they generate, npj Quantum Information 9, 96 (2023).
- [47] J. Wallman, C. Granade, R. Harper, and S. T. Flammia, Estimating the coherence of noise, New Journal of Physics 17, 113020 (2015).
- [48] A. Carignan-Dugas, J. J. Wallman, and J. Emerson, Bounding the average gate fidelity of composite channels using the unitarity, New Journal of Physics 21, 053016 (2019).
- [49] A. A. Mele, Introduction to haar measure tools in quantum information: A beginner's tutorial, arXiv preprint arXiv:2307.08956 (2023).

Supplementary Materials for: Symmetric Clifford twirling for cost-optimal quantum error mitigation in early FTQC regime

CONTENTS

S1. Scheme of early fault-tolerant quantum computing	7
S2. Comparison of the sampling overhead of QEM methods	ç
S3. Distance between Pauli noise and global white noise	11
S4. k-sparse symmetric Clifford twirling	12
S5. Unitarity and the average noise strength	14
S6. White-noise approximation in the early-FTQC regime	15
S7. Proof of Theorem 2 in the main text	16
S8. Proof of Theorem S1	18

S1. SCHEME OF EARLY FAULT-TOLERANT QUANTUM COMPUTING

As we have mentioned in the main text, we envision that, in the early FTQC era, the logical error rate is significantly suppressed by quantum error correction such that we may implement deep quantum circuit with polynomial depth. In the following, we argue that additional Clifford operation for symmetric Clifford twirling does not increase the error in the early FTQC or FTQC regime, in particular when the circuit depth is of $\Omega(n)$. We assume that entangling operations are done via the lattice surgery and non-Clifford gates are implemented via gate teleportation. In such a setup, three main logical error source can be understood as summation of three terms: the decoding error, distillation error, and the gate synthesis error.

The decoding error indicates the error due to the limitation of the error correction code and decoding algorithm. When we employ an error correction code of distance d, no matter how good the decoding algorithm is, we inevitably have logical error of $p_{\rm dec} = O((p/p_{\rm th})^{\frac{d+1}{2}})$ where p is the physical error rate and $p_{\rm th}$ is the threshold of the code. For instance, in the case of surface code, it is commonly estimated that $p_{\rm dec} = 0.1(p/p_{\rm th})^{\frac{d+1}{2}}$ with $p_{\rm th} = 0.01$ [40–42] and therefore we have $p_{\rm dec} = 10^{-8}$ for $p = 10^{-3}$ and d = 13, for instance. When we perform multi Pauli measurement that involves k logical qubits including logical ancilla patches, the logical error is multiplied by a factor of k. Therefore, if we perform R rounds of logical Pauli measurement that involves k_r logical qubits at the r-th round, the total decoding error can be estimated as

$$N_{\text{dec}} = p_{\text{dec}} \sum_{r=1}^{R} k_r, \tag{S1}$$

where $\sum_{r} k_r$ is referred to as the circuit volume in the literature.

The distillation error roots from insufficiency of the magic state distillation. For instance, in the context of preparing the magic state for T gates, it is common to utilize the 15-to-1 protocol that is essentially an error detection using Reed-Muller code that allows transversal implementation of the T gate [10]. Reflecting the fact that the code is a [15,1,3] code, the protocol suppresses the error up to the cubic order and outputs a single magic state of error rate $35p^3$, using 15 noisy magic states of error rate p. In general, by choosing [n',k',d'] codes that allows transversal implementation of T gates, one can suppress the distillation error up to d'th order. The total of the distillation error can be written as

$$N_{\rm dis} = p_{\rm dis} n_T, \tag{S2}$$

where $p_{\rm dis}$ is the error rate of the distilled magic state and n_T is the number of $\pi/8$ rotations (or T count) in the circuit. If multiple types of magic states are employed, we can simply sum over the error from each of them.

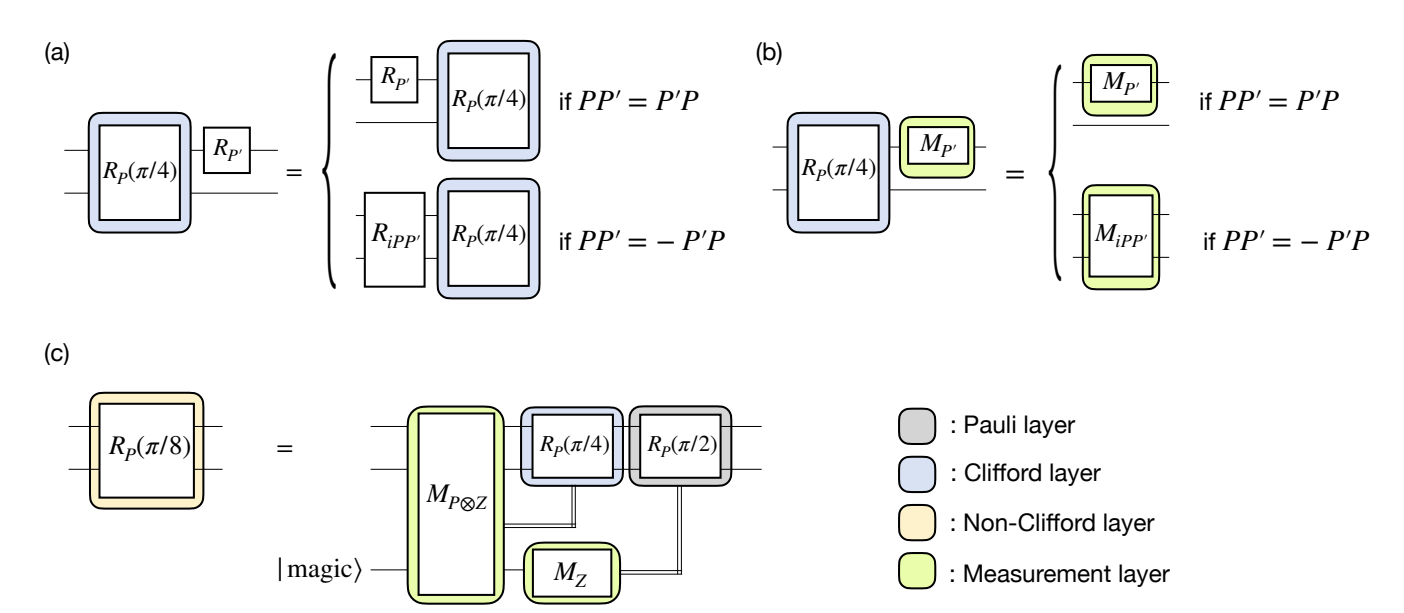


FIG. S1. Gate conjugation rule discussed in Ref. [40]. (a) Commutation rule of Pauli rotation gates. Here, $R_P(\theta)$ denotes the Pauli rotation $e^{iP\theta}$. (b) Absorption of $\pi/4$ rotation gate into measurement. (c) Implementation of $\pi/8$ rotation of Pauli operator P via gate teleportation of $|\text{magic}\rangle = |0\rangle + e^{i\pi/4}|1\rangle$. Note that $|\text{magic}\rangle$ does not rely on R_P as long as the rotation angle is $\pi/8$, which simplifies the magic state distillation protocol.

Finally, the synthesis error indicates the coherent error that arises when we decompose a given arbitrary gate into a sequence of fault-tolerant gates that only constitute discrete set. For instance, when one employs the Clifford+T gate set, a Pauli rotation gate is typically decomposed into a sequence that consists of H, S, and T gates. The gate complexity to approximate the target unitary up to accuracy of ϵ is $O(\text{polylog}(1/\epsilon))$, which is considered to be non-negligible when the number of T gates are limited as in early FTQC era. However, the synthesis error is distinct from other two errors in a sense that it can be characterized completely without quantum measurement. This has lead to several proposals that suppress the synthesis error up to quadratic or cubic order without increasing circuit depth at all [34, 43, 44]. For the sake of the discussion below, let us define the total contribution from synthesis error as N_{syn} . In the case when the quantum circuit consists of Clifford gates and Pauli rotations, we can rewrite it as

$$N_{\text{syn}} = p_{\text{rot}} N_{\text{rot}},\tag{S3}$$

where p_{rot} is the synthesis error per gate and N_{rot} is the number of rotation gates.

With all the contributions taken into account, the expected number of error in the quantum circuit per single run can be written as

$$N_{\rm err} = N_{\rm dec} + N_{\rm dis} + N_{\rm syn}.$$
 (S4)

When we run the quantum circuit, we design the entire protocol so that $N_{\rm err}=O(1)$, while we can arbitrarily choose how each error contributes to $N_{\rm err}$. In this work, we consider a situation where the number of physical qubit is limited to tens of thousands to hundreds of thousands. In such a situation, we may allow increasing the code distance d for each logical qubit, while we do not want to blow up the number of logical qubits. Since the number of data and ancilla logical qubits are typically determined from the problem itself, we shall aim to reduce the number of logical qubits for magic state factories. For instance, we may use the zero-level distillation that yields error of $100p^2$ with using only a single logical qubit [31], or may choose one round of magic state distillation that yields $p_{\rm dis} = O(p^2)$. In the case of $p = 10^{-3}$, we typically have $p_{\rm dis} = 10^{-4}$ or 10^{-5} . Note that this is orders of magnitudes higher than the decoding error assuming d = 11 or d = 13, and thus give a good justification to the assumption that the total error is dominated by the non-Clifford gates.

However, even if the contribution from the decoding error, or $N_{\rm dec}/N_{\rm err}$, is small, this does not directly imply that twirling Clifford operations can be added as much as desired. To argue the harmlessness of twirling operations, we must be aware that Clifford operations themselves are not implemented as actual gates. It was proposed by Litinski that, when we employ lattice-surgery-based scheme for FTQC using surface codes, we shall follow the rules shown in Fig. S1 to obtain a compiled circuit as depicted in Fig. S2. Namely, all the non-Clifford Pauli rotations must be

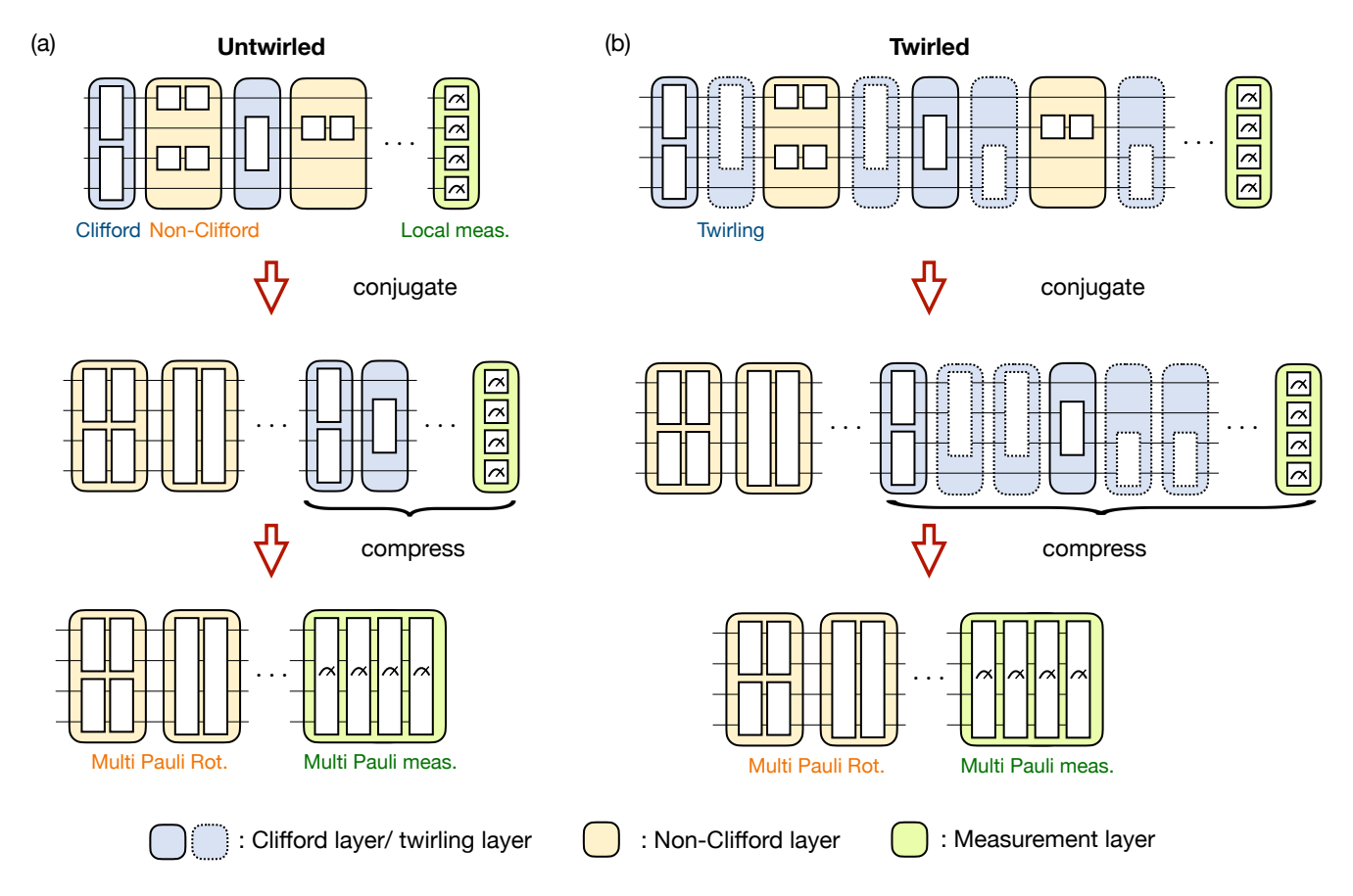


FIG. S2. Compilation of (a) untwirled and (b) twirled quantum circuit assuming FTQC with lattice surgery and magic state gate teleportation. In the first stage, we conjugate the non-Clifford Pauli rotations through the Clifford layers so that all non-Clifford layers are placed before the Clifford layers. In the second stage, the Clifford layers are absorbed into the measurement layer.

conjugated backwards to the beginning of the circuit, and the Clifford operations must be conjugated forward so that it can be merged with the measurement. When the circuit is sufficiently deep, e.g. $\Omega(n)$ depth for n-qubit simulation, then most of the multi Pauli rotations and multi Pauli measurements involve O(n) logical qubits. Therefore, even if we add twirling operations as shown in Fig. S2(b), it only conjugates the measured Pauli operators; the circuit volume is not significantly affected, and thus the contribution to the total error can be expected to be small.

S2. COMPARISON OF THE SAMPLING OVERHEAD OF QEM METHODS

In this section, we discuss the sampling overhead of some quantum error mitigation (QEM) methods and compare them with the theoretical lower bound proposed in Ref. [25].

Let us focus on the scenario where we aim to estimate the expectation value of an observable O for the n-qubit noiseless quantum state

$$\rho_{\text{ideal}} := \mathcal{C}_{L+1} \circ \mathcal{U} \circ \mathcal{C}_L \circ \cdots \circ \mathcal{U} \circ \mathcal{C}_1(\rho_0), \tag{S5}$$

but we only have access to the noisy quantum state

$$\rho_{\text{noisy}} := \mathcal{C}_{L+1} \circ \mathcal{N} \circ \mathcal{U} \circ \mathcal{C}_L \circ \cdots \circ \mathcal{N} \circ \mathcal{U} \circ \mathcal{C}_1(\rho_0), \tag{S6}$$

where $C_l(\cdot) := C_l \cdot C_l^{\dagger}$ is the l-th Clifford layer, $\mathcal{U}(\cdot) := U \cdot U^{\dagger}$ is the non-Clifford layer, \mathcal{N} is the noise layer, ρ_0 is the initial state, and L represents the number of the noisy non-Clifford layers. Here, for simplicity, we assume that O is a traceless observable satisfying $-I \le O \le I$ and \mathcal{N} is a Pauli noise given by $\mathcal{N} := (1 - p_{\text{err}})\mathcal{I} + \sum_i p_i \mathcal{E}_{P_i}$, where Pauli error $\mathcal{E}_{P_i}(\cdot) := P_i \cdot P_i$ occurs with probability p_i with $p_{\text{err}} := \sum_i p_i$ being the error probability.

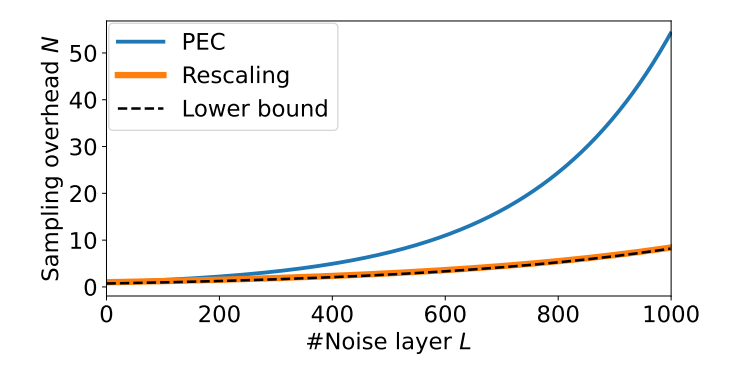


FIG. S3. Comparison of the sampling overhead N for probabilistic error cancellation [16–18] (blue line) and the rescaling method (orange line) when $p_{\rm err} = 10^{-3}$ and $n \gg 1$. The sampling overhead of the rescaling method is not only quadratically improved from probabilistic error cancellation, but also saturates the lower bound proposed in Ref. [25] (dotted line).

By utilizing QEM techniques, we can construct an estimator for $tr[\rho_{ideal}O]$ solely from multiple executions of the noisy logical circuit (with some modifications). Recently, a lower bound on the sampling overhead N, which is a multiplicative factor in the number of circuit executions needed to achieve the same estimation accuracy as in the noiseless case, has been established as

$$N \ge \left(\frac{4^n \nu(\mathcal{N}^{-1}) - 1}{4^n - 1}\right)^L - \frac{2^n - 2}{4^n - 1},\tag{S7}$$

where $\nu(\mathcal{N}^{-1}) = \operatorname{tr}[I \otimes \mathcal{N}^{-1}(|\Gamma\rangle\langle\Gamma|)^2]/4^n$ represents the purity of the Choi matrix of \mathcal{N}^{-1} with $|\Gamma\rangle = \sum_i |i\rangle|i\rangle$ (Theorem S1 of Ref. [25]). When we assume that \mathcal{N} is a Pauli noise, we can calculate $\nu(\mathcal{N}^{-1})$ as $\nu(\mathcal{N}^{-1}) = 1 + 2p_{\text{err}} + O(p_i^2)$. Consequently, we obtain

$$N \gtrsim \left(1 + \frac{4^n}{4^n - 1} 2p_{\text{err}}\right)^L - \frac{2^n - 2}{4^n - 1}$$
 (S8)

as the lower bound on the sampling overhead necessary to mitigate Pauli errors, considering up to the first degree of the error probability.

This lower bound can be saturated when we can convert noise layer \mathcal{N} into the global white noise defined as

$$\mathcal{N}_{\text{wn},p_{\text{err}}} := (1 - p_{\text{err}})\mathcal{I} + p_{\text{err}} \mathbb{E}_i [\mathcal{E}_{P_i}]$$
 (S9)

where each n-qubit Pauli error occurs with equal probability of $(4^n-1)^{-1}p_{\rm err}$. Global white noise can also be expressed as

$$\mathcal{N}_{\text{wn},p_{\text{err}}}(\cdot) = \left(1 - \frac{4^n}{4^n - 1}p_{\text{err}}\right) \cdot + \frac{4^n}{4^n - 1}p_{\text{err}}I,\tag{S10}$$

so we can mitigate errors by simply rescaling the noisy expectation value as

$$\left(1 - \frac{4^n}{4^n - 1} p_{\text{err}}\right)^{-L} \operatorname{tr}[\rho_{\text{noisy}} O] = \operatorname{tr}[\rho_{\text{ideal}} O] \tag{S11}$$

with a sampling overhead of $N = \left(1 - \frac{4^n}{4^n - 1} p_{\text{err}}\right)^{-2L}$. This rescaling method represents a quadratic improvement over probabilistic error cancellation, whose sampling overhead is $N \sim (1 + 2p_{\text{err}})^{2L}$ [16, 18]. Additionally, this sampling overhead saturates the lower bound given by Eq. (S8) when p_{err} is small and n is large. Thus, we can conclude that the rescaling method is a cost-optimal QEM method (see Fig. S3).

While the rescaling method effectively mitigate errors with minimal sampling overhead, this overhead still grows exponentially with the number of noisy layer L. Therefore, a practical scenario arises when the total error rate $p_{\text{tot}} := p_{\text{err}}L$ can be regarded as a constant value. In this situation, if p_{err} is small and n is large, the sampling overhead can be approximated as a constant value represented as $N \sim e^{2p_{\text{tot}}}$.

We note that the lower bound described in Eq. (S8) applies solely to QEM methods that do not utilize additional ancilla qubits or implement mid-circuit measurements. Indeed, by introducing logical ancilla qubits, it is known that we can reduce the sampling overhead below the lower bound. However, the use of logical ancilla qubits may impose an extra burden in terms of the space overhead, which may not be desirable when the number of qubits is scarce. Therefore, we focus on the QEM methods that do not use ancilla qubits and regard the rescaling method as a cost-optimal QEM method.

S3. DISTANCE BETWEEN PAULI NOISE AND GLOBAL WHITE NOISE

In the main text, we explained that we can exponentially reduce the distance between Pauli noise and global white noise by performing symmetric Clifford twirling. In this section, we clarify the precise meaning of this statement by introducing a 2-norm for the normalized error probabilities.

As the distance between Pauli noise $\mathcal{N} = (1 - p_{\text{err}})\mathcal{I} + \sum_i p_i \mathcal{E}_{P_i}$ with error probability p_{err} and the global white noise $\mathcal{N}_{\text{wn},p_{\text{err}}} = (1 - p_{\text{err}})\mathcal{I} + p_{\text{err}}\mathbb{E}_i[\mathcal{E}_{P_i}]$, we define 2-norm v of the normalized error probabilities as

$$v := \sqrt{\sum_{i} \left(\frac{p_i}{p_{\text{err}}} - \frac{1}{4^n - 1}\right)^2} = \sqrt{\sum_{i} \left(\frac{p_i}{p_{\text{err}}}\right)^2 - \frac{1}{4^n - 1}}.$$
 (S12)

This distance measure v is valuable as it helps bound the bias between the ideal and the rescaled noisy expectation values (see Corollary S1). By analyzing how v changes through symmetric Clifford twirling, we can assess the efficacy of this technique in QEM.

Let us first calculate v for Pauli-X noise acting on the first qubit, represented as $(1-p_{\rm err})\mathcal{I}+p_{\rm err}\mathcal{E}_{{\rm X}\otimes{\rm I}^{\otimes(n-1)}}$. Since it consists of a single Pauli error, the sum of squares of normalized error probability satisfies $\sum_i (p_i/p_{\rm err})^2 = 1$. Therefore, we can calculate v as v=1 up to the leading order of n. Meanwhile, from Theorem 1 in the main text, symmetric Clifford twirling scrambles the noise into the noise represented as

$$(1 - p_{\text{err}})\mathcal{I} + p_{\text{err}} \underset{\substack{Q_1 \in \{X,Y\}\\Q_2 \in \mathcal{P}_{n-1}}}{\mathbb{E}} [\mathcal{E}_{Q_1 \otimes Q_2}]. \tag{S13}$$

The scrambled noise is now a noise where $2 \times 4^{n-1}$ Pauli errors occur with equal probability, so the sum of squares of normalized error probability satisfies $\sum_{i} (p_i/p_{\rm err})^2 = 2/4^n$. Therefore, we can calculate v as $v = 2^{-n}$ up to the leading order of n. Thus, by performing symmetric Clifford twirling, we can decrease the distance v from 1 to 2^{-n} .

Next, we consider Pauli-Z noise acting on the first qubit represented as $(1 - p_{\text{err}})\mathcal{I} + p_{\text{err}}\mathcal{E}_{Z\otimes I^{\otimes (n-1)}}$. From Theorem 1 in the main text, we cannot twirl the Pauli-Z noise, so the distance is v = 1 whether or not we implement symmetric Clifford twirling.

Finally, we consider depolarizing noise acting on the first qubit represented as $(1 - p_{\text{err}})\mathcal{I} + p_{\text{err}}(\mathcal{E}_{X \otimes I^{\otimes (n-1)}} + \mathcal{E}_{Y \otimes I^{\otimes (n-1)}}) + \mathcal{E}_{Z \otimes I^{\otimes (n-1)}})/3$. Since three kinds of Pauli noise occur with equal probability, the sum of squares of normalized error probability satisfies $\sum_{i} (p_i/p_{\text{err}})^2 = 1/3$. Therefore, we can calculate v as $v = 1/\sqrt{3}$ up to the leading order of n. When we twirl the depolarizing noise using symmetric Clifford operators, the noise is scrambled to be

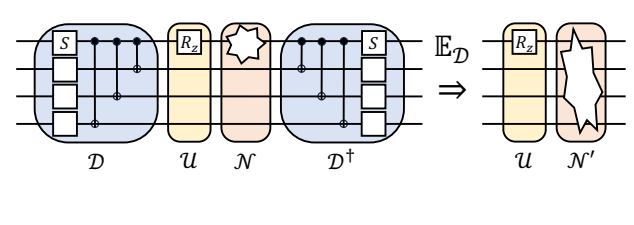
$$(1 - p_{\text{err}})\mathcal{I} + p_{\text{err}}\left(\frac{1}{3}\mathcal{E}_{\mathbf{Z}\otimes\mathbf{I}^{\otimes(n-1)}} + \frac{2}{3} \underset{Q_2 \in \mathcal{P}_{n-1}}{\mathbb{E}} [\mathcal{E}_{Q_1 \otimes Q_2}]\right), \tag{S14}$$

because the Pauli-X and Y noise is scrambled but the Pauli-Z noise remains unchanged. Since the sum of squares of normalized error probability of this noise satisfies $\sum_i \left(p_i/p_{\rm err}\right)^2 = 1/9 + 4/9 \times 2/4^n$, we can calculate v as v=1/3 up to the leading order of n. Thus, by performing symmetric Clifford twirling, we can decrease the distance v from $1/\sqrt{3}$ to 1/3 because the Pauli-X and Y noise is scrambled but the Pauli-Z noise remains unchanged.

We note that the well-used diamond norm normalized by the error probability is the 1-norm of normalized error probabilities [45]:

$$\|\mathcal{N} - \mathcal{N}_{\text{wn}, p_{\text{err}}}\|_{\Diamond}/p_{\text{err}} = \sum_{i} \left| \frac{p_{i}}{p_{\text{err}}} - \frac{1}{4^{n} - 1} \right|. \tag{S15}$$

(a) Symmetric Clifford twirling



(b) 2-sparse symmetric Clifford twirling

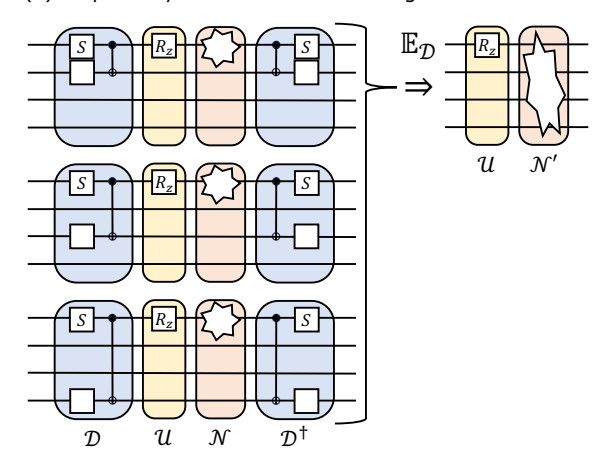


FIG. S4. Schematic figure of (a) symmetric Clifford twirling and (b) 2-sparse symmetric Clifford twirling. While symmetric Clifford twirling aims to propagate noise to all n-1 idling qubits, 2-sparse symmetric Clifford twirling propagates noise only to a single idling qubit, which is randomly selected for each circuit execution.

S4. k-SPARSE SYMMETRIC CLIFFORD TWIRLING

In Sec. S1, we explained that adding symmetric Clifford unitary $D \in \mathcal{G}_{n,\mathcal{Q}_U}$ to the logical circuit primarily modifies the multi-qubit Pauli rotation layer and the multi-qubit Pauli measurements at the beginning and end of the circuit. However, when considering different architectures such as those allowing transversal implementation of the CNOT gate [8], it may be necessary to apply multi-qubit Clifford unitary D directly to the circuit using CNOT and single-qubit Clifford gates. In such a situation, the implementation of the multi-qubit Clifford unitary D can require a depth of 1.5n + O(1) under all-to-all connectivity in the worst case [46], potentially leading to a significant amount of decoding error as the number of logical qubits increases. To address this issue, we need to consider twirling the noise using sparse symmetric Clifford operations acting on a small number of qubits. In this section, we introduce k-sparse symmetric Clifford twirling, which is a symmetric Clifford twirling using only a k-local symmetric Clifford operation. We show here that we can still scramble the noise to a noise polynomially close to the global white noise with k-sparse symmetric Clifford twirling.

Let us consider the scenario where the non-Clifford layer \mathcal{U} consists of either the T gate or the Pauli-Z rotation gate $R_z(\theta)$ applied to the first qubit, and the noise layer \mathcal{N} introduces Pauli-X or Y noise affecting solely the first qubit as in the main text. In this particular case, the Pauli-X and Y noise can be scrambled as

$$\mathscr{T}_{\mathcal{Q}_{U}}(\mathcal{E}_{P\otimes \mathbf{I}^{\otimes n-1}}) = \mathbb{E}_{D\in\mathcal{G}_{n,\mathcal{Q}_{U}}}[\mathcal{D}^{\dagger}\circ\mathcal{E}_{P\otimes \mathbf{I}^{\otimes n-1}}\circ\mathcal{D}] = \mathbb{E}_{\substack{Q_{1}\in\{\mathbf{X},\mathbf{Y}\}\\Q_{2}\in\mathcal{P}_{n-1}}}[\mathcal{E}_{Q_{1}\otimes Q_{2}}]$$
(S16)

by using all of the symmetric Clifford unitaries $D \in \mathcal{G}_{n,\mathcal{Q}_U}$, including the global ones, as discussed in Theorem 1 in the main text.

While implementing arbitrary symmetric Clifford operations requires a depth of 1.5n + O(1) under all-to-all connectivity in the worst case [46], sampling from all elements in $\mathcal{G}_{n,\mathcal{Q}_U}$ is not necessary to achieve the twirled noise as shown in Eq. (S16). Instead, the noise can be propagated probabilistically to n-1 idling qubits, and then locally twirled using single-qubit Clifford operations. This can be done by constructing $D \in \mathcal{G}_{n,\mathcal{Q}_U}$ in the following way:

- 1. For $i = 2, \dots, n$, perform the following operation.
 - (a) Add CNOT gate where the first qubit acts as the control qubit and the *i*-th qubit is the target qubit with probability 3/4.
 - (b) Randomly and uniformly sample a single-qubit Clifford gate.
 - (c) Add the sampled gate to the *i*-th qubit.
- 2. Add S gate to the first qubit with probability 1/2.

TABLE S1. Distance v between the Pauli noise affecting the first qubit with error probability $p_{\rm err}$ and global white noise $\mathcal{N}_{{\rm wn},p_{\rm err}}$. his table presents values of v for three scenarios: the original noise, after applying symmetric Clifford twirling, and after applying k-sparse symmetric Clifford twirling. Here, we only consider the leading order of n.

Noise model	Pauli Z	depolarizing	Pauli X or Y
Original noise	1	$1/\sqrt{3}$	1
Symmetric Clifford twirling	1	1/3	2^{-n}
k-sparse symmetric Clifford twirling	1	1/3	$1/\sqrt{2(3n)^{k-1}}$

This strategy requires up to n-1 CNOT gates and can be implemented with $\log(n)$ depth using a tree-like structure of CNOT layers [38]. However, this simplified approach still involves O(n) gates per noise layer, potentially leading to a non-negligible amount of decoding error as the number of logical qubits increases.

Instead of propagating the noise to all n-1 idling qubits, we can economize the number of gates by limiting noise propagation to up to k-1 qubits. As an example of such a strategy, let us consider constructing D in the following way.

- 1. Sample $k' \in \{0, \dots, k-1\}$ with probability $3^{k'} \binom{n-1}{k'} / \sum_{k''=0}^{k-1} 3^{k''} \binom{n-1}{k''}$.
- 2. Randomly and uniformly select k' qubit from the idling n-1 qubits.
- 3. Add k' CNOT gates where the first qubit acts as the control qubit and the selected k' qubits are the target qubits.
- 4. Randomly and uniformly sample k' single-qubit Clifford gates.
- 5. Apply each sampled single-qubit Clifford gate to the corresponding selected k' qubit.
- 6. Add S gate to the first qubit with probability $\frac{1}{2}$.

Step 1 in the above construction determines the number of qubits to which the noise is propagated, where $\binom{n-1}{k'}$ is a binomial coefficient and $3^{k'}\binom{n-1}{k'}$ represents the number of (n-1)-qubit Pauli operators with Pauli weight k'. Here, the Pauli weight refers to the number of qubits on which a Pauli operator non-trivially acts. Step 2 selects which k' qubit to propagate the noise, and step 3 propagates the noise to the selected qubits. Finally, we locally scramble the noise with steps 4 to 6.

Since the constructed $D \in \mathcal{G}_{n,\mathcal{Q}_U}$ in the above way affects at most k qubits, we refer to the twirling using such D as k-sparse symmetric Clifford twirling. This construction method scrambles the noise to the uniform average of Pauli noise with Pauli weights up to k-1. Consequently, the effect of k-sparse symmetric Clifford twirling can be mathematically described as:

$$\mathscr{T}_{Q_U}^{k\text{-sparse}}(\mathcal{E}_{P\otimes \mathrm{I}^{\otimes n-1}}) = \mathbb{E}_{D\in\mathcal{G}_{n,Q_U}}^{k\text{-sparse}}[\mathcal{D}^{\dagger}\circ\mathcal{E}_{P\otimes \mathrm{I}^{\otimes n-1}}\circ\mathcal{D}] = \underset{Q_1\in\{\mathrm{X},\mathrm{Y}\}}{\mathbb{E}}_{Q_1\in\{\mathrm{X},\mathrm{Y}\}}[\mathcal{E}_{Q_1\otimes Q_2}]$$
(S17)

where $\mathbb{E}_{D\in\mathcal{G}_{n,\mathcal{Q}_U}}^{k\text{-sparse}}$ represents the average over the above construction of D and $w(Q_2)$ denotes the Pauli weight of Q_2 . If we apply k-sparse symmetric Clifford twirling to Pauli-X noise acting on the first qubit, represented as $(1-p_{\text{err}})\mathcal{I}+p_{\text{err}}\mathcal{E}_{X\otimes I^{\otimes (n-1)}}$, we obtain

$$(1 - p_{\text{err}})\mathcal{I} + p_{\text{err}} \underset{\substack{Q_1 \in \{X, Y\}\\Q_2 \in \mathcal{P}_{n-1}, w(Q_2) \le k-1}}{\mathbb{E}} [\mathcal{E}_{Q_1 \otimes Q_2}].$$
 (S18)

The twirled noise is the uniform average of $2\sum_{k''=0}^{k-1} 3^{k''} {n-1 \choose k''} \sim 2(3n)^{k-1}$ types of Pauli noise, so the sum of squares of normalized error probability satisfies $\sum_i (p_i/p_{\rm err})^2 \sim 2^{-1}(3n)^{-k+1}$. Therefore, we can calculate the distance v from the global white noise as $v=1/\sqrt{2(3n)^{k-1}}$ up to the leading order of n. This means that, by performing k-sparse symmetric Clifford twirling, we can scramble Pauli-X or Y noise to a noise that is polynomially close to the global white noise (see Table S1). Especially when we consider the situation where Pauli-Z noise remains, we can achieve the same performance as in symmetric Clifford twirling. This is even true for the 2-sparse twirling, where we only need a single CNOT gate to construct $D \in \mathcal{G}_{n,\mathcal{Q}_U}$ to perform twirling. Thus, we can conclude that the k-sparse symmetric Clifford twirling provides a practical approach to noise mitigation, achieving substantial noise scrambling with minimal hardware overhead.

S5. UNITARITY AND THE AVERAGE NOISE STRENGTH

In order to introduce the notion of white-noise approximation [29], let us define unitarity and the average noise strength for the noise layer \mathcal{N} in this section.

Let $\mathcal{N} = \sum_i E_i \cdot E_i^{\dagger}$ be a unital noise. Then, we define the unitarity u [29, 47, 48] and the average noise strength s of the noise channel as

$$u = \frac{2^n}{2^n - 1} \left(\mathbb{E}_{V \sim \mu_H} \left[\text{tr} \left[\mathcal{N}(V | \psi \rangle \langle \psi | V^{\dagger})^2 \right] \right] - \frac{1}{2^n} \right), \tag{S19}$$

$$s = \frac{2^n}{2^n - 1} \left(\mathbb{E}_{V \sim \mu_H} \left[\text{tr} \left[V | \psi \rangle \langle \psi | V^{\dagger} \mathcal{N} (V | \psi \rangle \langle \psi | V^{\dagger}) \right] \right] - \frac{1}{2^n} \right), \tag{S20}$$

where $\mathbb{E}_{V \sim \mu_H}$ denotes the average over the Haar measure μ_H on the unitary group. The unitarity u is the expected purity of the output state under a random choice of input state, which has a minimum value of 0 and a maximum value of 1. The average noise strength s represents the noise strength of the twirled noisy channel as $\mathbb{E}_{V \sim \mu_H}[V^{\dagger} \mathcal{N}(V \cdot V^{\dagger})V] = s \cdot + (1-s)I/2^n$ [26]. We can represent the unitarity u and the average noise strength s using the Kraus operators of $\mathcal{N} = \sum_i E_i \cdot E_i^{\dagger}$ by using the 2-moment operator [49]

$$\mathcal{M}(\mathbb{O}) = \mathbb{E}_{V \sim \mu_H}[V^{\otimes 2} \mathbb{O} V^{\dagger \otimes 2}] \tag{S21}$$

$$= \frac{2^{2n}\operatorname{tr}[\mathbb{O}] - 2^{n}\operatorname{tr}[\mathbb{O}\mathbb{F}]}{2^{2n} - 1} \frac{\mathbb{I}}{2^{2n}} + \frac{2^{n}\operatorname{tr}[\mathbb{O}\mathbb{F}] - \operatorname{tr}[\mathbb{O}]}{2^{2n} - 1} \frac{\mathbb{F}}{2^{n}}, \tag{S22}$$

where \mathbb{O} is an arbitrary operator, \mathbb{I} is the identity operator and \mathbb{F} is the swap operator on the two copies of 2^n -dimensional Hilbert space. By using the 2-moment operator $\mathcal{M}(\mathbb{O})$, we obtain

$$u = \frac{2^n}{2^n - 1} \left(\sum_{ij} \operatorname{tr} \left[(E_i \otimes E_j) \mathcal{M}((|\psi\rangle\langle\psi|)^{\otimes 2}) (E_i^{\dagger} \otimes E_j^{\dagger}) \mathbb{F} \right] - \frac{1}{2^n} \right)$$
 (S23)

$$= \frac{2^n}{2^n - 1} \left(\sum_{ij} \text{tr} \left[(E_i \otimes E_j) \left(\frac{2^{2n} - 2^n}{2^{2n} - 1} \frac{\mathbb{I}}{2^{2n}} + \frac{1}{2^n + 1} \frac{\mathbb{F}}{2^n} \right) (E_i^{\dagger} \otimes E_j^{\dagger}) \mathbb{F} \right] - \frac{1}{2^n} \right)$$
(S24)

$$= \frac{2^n}{2^n - 1} \left(\frac{2^n - 1}{2^n (2^{2n} - 1)} \sum_{ij} \operatorname{tr}[E_i E_i^{\dagger} E_j E_j^{\dagger}] + \frac{1}{2^n (2^n + 1)} \sum_{ij} \operatorname{tr}|[E_i E_j^{\dagger}]|^2 - \frac{1}{2^n} \right)$$
(S25)

$$= \frac{\sum_{ij} |\text{tr}[E_i E_j^{\dagger}]|^2 - 1}{4^n - 1}$$
 (S26)

for the unitarity u and

$$s = \frac{2^n}{2^n - 1} \left(\sum_i \operatorname{tr} \left[(E_i \otimes I) \mathcal{M}((|\psi\rangle\langle\psi|)^{\otimes 2}) (E_i^{\dagger} \otimes I) \mathbb{F} \right] - \frac{1}{2^n} \right)$$
 (S27)

$$= \frac{2^n}{2^n - 1} \left(\sum_i \text{tr} \left[(E_i \otimes I) \left(\frac{2^{2n} - 2^n}{2^{2n} - 1} \frac{\mathbb{I}}{2^{2n}} + \frac{1}{2^n + 1} \frac{\mathbb{F}}{2^n} \right) (E_i^{\dagger} \otimes I) \mathbb{F} \right] - \frac{1}{2^n} \right)$$
 (S28)

$$= \frac{2^n}{2^n - 1} \left(\frac{2^n - 1}{2^n (2^{2n} - 1)} \sum_i \operatorname{tr}[E_i E_i^{\dagger}] + \frac{1}{2^n (2^n + 1)} \sum_i |\operatorname{tr}[E_i]|^2 - \frac{1}{2^n} \right)$$
 (S29)

$$= \frac{\sum_{i} |\text{tr}[E_i]|^2 - 1}{4^n - 1} \tag{S30}$$

for the average noise strength s, where we used $\sum_i E_i E_i^{\dagger} = I$ for unital noise. Thus, for Pauli noise $\mathcal{N}(\cdot) = (1 - p_{\text{err}}) \cdot + \sum_i p_i P_i \cdot P_i$, these parameters can be represented as

$$u = 1 - \frac{4^n}{4^n - 1} 2p_{\text{err}} + \frac{4^n}{4^n - 1} \left(p_{\text{err}}^2 + \sum_i p_i^2 \right), \tag{S31}$$

$$s = 1 - \frac{4^n}{4^n - 1} p_{\text{err}}.$$
 (S32)

S6. WHITE-NOISE APPROXIMATION IN THE EARLY-FTQC REGIME

In the realm of NISQ computing, it has been demonstrated that the effective noise of random quantum circuits consisting of noisy 2-qubit gates can be approximated as the global white noise [29]. This approximation, known as the white-noise approximation, arises from the scrambling of local errors to other qubits due to the randomness of gates. In the early FTQC regime, the primary source of errors is not multi-qubit Clifford gates, but rather (potentially single-qubit) non-Clifford gates. Conversely, as long as the gate is Clifford, we can execute multi-qubit operations with negligible errors. This implies that the Clifford layer $C_l(\cdot) = C_l \cdot C_l^{\dagger}$ can, in theory, represent any n-qubit Clifford unitary. Thus, if we want to capture the typical behavior of the logical circuits, we may consider the case where C_l is randomly and uniformly drawn from the n-qubit Clifford group \mathcal{G}_n . In such a scenario, local noise is anticipated to be more effectively scrambled to other qubits compared to NISQ circuits, where randomness arises from noisy 2-qubit gates. Therefore, we can assert that the white-noise approximation is better suited for the early FTQC regime than the NISQ regime.

As in Sec. S2, we focus on the scenario where we aim to estimate the expectation value of an observable O for the n-qubit noiseless quantum state

$$\rho_{\text{ideal}} := \mathcal{C}_{L+1} \circ \mathcal{U} \circ \mathcal{C}_L \circ \cdots \circ \mathcal{U} \circ \mathcal{C}_1(\rho_0), \tag{S33}$$

but we only have access to the noisy logical quantum state

$$\rho_{\text{noisy}} := \mathcal{C}_{L+1} \circ \mathcal{N} \circ \mathcal{U} \circ \mathcal{C}_L \circ \cdots \circ \mathcal{N} \circ \mathcal{U} \circ \mathcal{C}_1(\rho_0), \tag{S34}$$

where $C_l(\cdot) := C_l \cdot C_l^{\dagger}$ is the *l*-th Clifford layer, $U(\cdot) := U \cdot U^{\dagger}$ is the non-Clifford layer, \mathcal{N} is the noise layer, ρ_0 is the initial state, and L represents the number of the noisy non-Clifford layers. Here, for simplicity, we assume that O is a traceless observable satisfying $-I \leq O \leq I$ and \mathcal{N} is a unital noise.

When we assume white-noise approximation, we can estimate the ideal expectation value $\operatorname{tr}[\rho_{\text{ideal}}O]$ by rescaling the noisy expectation value $\operatorname{tr}[\rho_{\text{noisy}}O]$ by some factor R. As the performance of white-noise approximation in the early FTQC regime for mitigating errors, we derive the following theorem by utilizing the discussion of Sec. 5.2 of Ref. [29].

Theorem S1. Let each Clifford gate C_l be drawn randomly and uniformly from the n-qubit Clifford group \mathcal{G}_n . Then, the noisy expectation value rescaled by the constant factor $R = (s/u)^L$ satisfies

$$\mathbb{E}_{C}[|R\mathrm{tr}[\rho_{\mathrm{noisy}}O] - \mathrm{tr}[\rho_{\mathrm{ideal}}O]|] \le \sqrt{\frac{2^{n} - 1}{2^{n} + 1}} \left(1 - \left(\frac{s^{2}}{u}\right)^{L}\right),\tag{S35}$$

where \mathbb{E}_C represents the uniform average over all Clifford unitary C_l over \mathcal{G}_n .

The sampling overhead N required to obtain the rescaled noisy expectation value $Rtr[\rho_{noisy}O]$ satisfies

$$N = \left(\frac{s}{u}\right)^L \sim \left(1 + \frac{4^n}{4^n - 1}p_{\text{err}}\right)^{2L} \tag{S36}$$

up to the first degree of p_{err} for Pauli noise $\mathcal{N} = (1 - p_{\text{err}})\mathcal{I} + \sum_i p_i \mathcal{E}_{P_i}$, where Pauli error $\mathcal{E}_{P_i}(\cdot) := P_i \cdot P_i$ occurs with probability p_i with $p_{\text{err}} = \sum_i p_i$ being the error probability. This saturates the lower bound on the sampling cost represented as Eq. (S8) when p_{err} is small and n is large, thus validating this rescaling method as a cost-optimal QEM method. This means that, besides converting local noise into global white noise through (symmetric) Clifford twirling, we can achieve cost-optimal QEM by assuming the white-noise approximation.

While the method described above allows us to mitigate errors with minimal sampling overhead, it still grows exponentially with L. Therefore, a practical scenario arises when the total error rate $p_{\text{tot}} := p_{\text{err}}L$ is maintained at a constant value, resulting in a constant sampling overhead approximated as $e^{2p_{\text{tot}}}$ for large L. In this case, we obtain the following corollary for Pauli noise:

Corollary S1. Let each Clifford gate C_l be randomly and uniformly drawn from the n-qubit Clifford group \mathcal{G}_n . Then, the noisy expectation value rescaled by the constant factor $R = (s/u)^L$ satisfies

$$\mathbb{E}_{C}[|R\mathrm{tr}[\rho_{\mathrm{noisy}}O] - \mathrm{tr}[\rho_{\mathrm{ideal}}O]|] \lesssim \frac{vp_{\mathrm{tot}}}{\sqrt{L}}$$
(S37)

for large L when $p_{tot} = p_{err}L$ is fixed to a constant value, where

$$v = \sqrt{\sum_{i} \left(\frac{p_i}{p_{\text{err}}} - \frac{1}{4^n - 1}\right)^2} \tag{S38}$$

represents the distance between the Pauli noise \mathcal{N} and the global white noise.

In the early FTQC regime, the logical error probability $p_{\rm err}$ is expected to decrease as hardware improves, allowing for an increase in the number of available noisy non-Clifford operations L for a fixed sampling overhead. Corollary S1 indicates that, in this scenario, the bias obtained through rescaling the noisy expectation value diminishes to 0, thereby confirming the effectiveness of the white-noise approximation as the hardware improves in the early FTQC regime. Even if L may not be sufficiently large to achieve the desired accuracy, we can reduce the average bias by reducing the parameter v using symmetric Clifford twirling.

While Corollary S1 assumes that each Clifford gate C_l is randomly sampled from the global n-qubit Clifford unitary, we anticipate a similar scaling behavior of $|R\text{tr}[\rho_{\text{noisy}}O] - \text{tr}[\rho_{\text{ideal}}O]| \sim O(vp_{\text{tot}}/\sqrt{L})$ holds even for simpler structured circuits, such as the Trotterized Hamiltonian simulation circuits demonstrated in the main text. Let us denote the Trotter step size as T. Then, we can represent L as L = 6nT for the 1D Heisenberg model and L = 12nT for the 2D Heisenberg model. In Fig. 4 in the main text, we observed that the average bias scales as $1/\sqrt{n}$ for the Trotterized Hamiltonian simulation circuits, indicating that it also scales as $1/\sqrt{L}$ for a fixed T. Furthermore, we observed that the scaling improves to 1/n by performing 2-sparse symmetric Clifford twirling, and this can be explained by the reduction of v from 1 to $O(1/\sqrt{n})$. Therefore, we expect similar results to Corollary S1 to hold for highly structured circuits in the early FTQC regime, where quantum circuits are sufficiently deep. It is worth noting that this property is specific to the early FTQC regime, as the white-noise approximation does not apply to shallow structured quantum circuits in the NISQ regime [37].

S7. PROOF OF THEOREM 2 IN THE MAIN TEXT

In this section, we present the proof of Theorem 2 in the main text, which we restate here for clarity.

Theorem 2. Let $P \in \mathcal{P}_n$ be an n-qubit Pauli operator, $\mathcal{E}_P(\cdot) = P \cdot P$ be the corresponding Pauli channel, and \mathcal{Q}_U be a Pauli subgroup. Let us decompose \mathcal{Q}_U as

$$Q_U = W^{\dagger}(\{I, X, Y, Z\}^{\otimes n_1} \otimes \{I, Z\}^{\otimes n_2} \otimes \{I\}^{\otimes n_3})W, \tag{S39}$$

where $W \in \mathcal{G}_n$ and $n_1, n_2, n_3 \in \mathbb{N}$ satisfying $n_1 + n_2 + n_3 = n$, and represent P as $P = W^{\dagger}(P_1 \otimes P_2 \otimes P_3)W$ up to phase, where $P_1 \in \mathcal{P}_{n_1}$, $P_2 \in \mathcal{P}_{n_2}$, and $P_3 \in \mathcal{P}_{n_3}$. Then, the Pauli channel scrambled through symmetric Clifford twirling $\mathcal{T}_{\mathcal{Q}_U}(\mathcal{E}_P)$ can be represented as:

(i) when $P_2 \notin \{I, Z\}^{\otimes n_2}$,

$$\mathscr{T}_{\mathcal{Q}_U}(\mathcal{E}_P) = \underset{\substack{Q_2 \in \{1,Z\}^{\otimes n_2} \\ Q_3 \in \mathcal{P}_{n_2}}}{\mathbb{E}} \left[\mathcal{E}_{W^{\dagger}(P_1 \otimes P_2 Q_2 \otimes Q_3)W} \right], \tag{S40}$$

(ii) when $P_2 \in \{I, Z\}^{\otimes n_2}$ and $P_3 \neq I^{\otimes n_3}$,

$$\mathcal{I}_{\mathcal{Q}_{U}}(\mathcal{E}_{P}) = \underset{\substack{Q_{2} \in \{\mathbf{I}, \mathbf{Z}\}^{\otimes n_{2}} \\ Q_{3} \in \mathcal{P}_{n_{3}} \setminus \{\mathbf{I}\}^{\otimes n_{3}}}}{\mathbb{E}} \left[\mathcal{E}_{W^{\dagger}(P_{1} \otimes Q_{2} \otimes Q_{3})W} \right], \tag{S41}$$

(iii) when $P_2 \in \{I, Z\}^{\otimes n_2}$ and $P_3 = I^{\otimes n_3}$,

$$\mathscr{T}_{\mathcal{Q}_U}(\mathcal{E}_P) = \mathcal{E}_P. \tag{S42}$$

Proof. In Ref. [28], it was shown that all elements in Q_U -symmetric Clifford group

$$\mathcal{G}_{n,\mathcal{Q}_U} := \{ C \in \mathcal{G}_n \mid \forall P \in \mathcal{Q}_U, \ [C,P] = 0 \}$$
(S43)

can be uniquely represented as

$$D = W^{\dagger}(I^{\otimes n_1} \otimes D_1) \times (I^{\otimes n_1} \otimes D_2 \otimes I^{\otimes n_3}) \times (I^{\otimes n_1} \otimes I^{\otimes n_2} \otimes D_3)W$$
(S44)

up to the phase. Here, D_1 is an $n_2 + n_3$ -qubit unitary represented as

$$D_1 = \Lambda_1(R_1) \cdots \Lambda_{n_2}(R_{n_2}), \tag{S45}$$

where $R_i \in \mathcal{P}_{n_3}$ is a Pauli operator acting on the last n_3 qubits and $\Lambda_i(R_i)$ is the controlled- R_i gate whose controlled qubit is the *i*-th qubit. D_2 is a element of $\{I,Z\}^{\otimes n_2}$ -symmetric Clifford group

$$D_2 \in \mathcal{G}_{n_2, \{I, Z\}^{\otimes n_2}} := \left\{ C \in \mathcal{G}_n \mid \forall R \in \{I, Z\}^{\otimes n_2}, \ [C, R] = 0 \right\}$$
 (S46)

and it can be uniquely represented as

$$D_2 = \prod_{\substack{i,j \in \{1,\dots,n_2\}\\i < j}} \operatorname{CZ}_{ij}^{\nu_{ij}} \prod_{i \in \{1,\dots,n_2\}} S_i^{\mu_i},$$
(S47)

where CZ_{ij} is the CZ gate acting on the *i*-th and *j*-th qubits, S_i is the S gate acting on *i*-th qubit, $\nu_{ij} \in \{0, 1\}$, and $\mu_i \in \{0, 1, 2, 3\}$. D_3 is an element of the Clifford group \mathcal{G}_{n_3} :

$$D_3 \in \mathcal{G}_{n_3}. \tag{S48}$$

Let us define the superchannels

$$\mathscr{T}_{1}(\mathcal{N}) := \mathbb{E}_{D_{1}} \left[\mathcal{E}_{\mathbf{I} \otimes n_{1} \otimes D_{1}}^{\dagger} \circ \mathcal{N} \circ \mathcal{E}_{\mathbf{I} \otimes n_{1} \otimes D_{1}} \right], \tag{S49}$$

$$\mathscr{T}_{2}(\mathcal{N}) := \mathbb{E}_{D_{2}} \left[\mathcal{E}_{\mathbf{I}^{\otimes n_{1}} \otimes D_{2} \otimes \mathbf{I}^{\otimes n_{3}}}^{\dagger} \circ \mathcal{N} \circ \mathcal{E}_{\mathbf{I}^{\otimes n_{1}} \otimes D_{2} \otimes \mathbf{I}^{\otimes n_{3}}} \right], \tag{S50}$$

$$\mathscr{T}_{3}(\mathcal{N}) := \mathbb{E}_{D_{3}} \left[\mathcal{E}_{\mathbf{I}^{\otimes n_{1}} \otimes \mathbf{I}^{\otimes n_{2}} \otimes D_{3}}^{\dagger} \circ \mathcal{N} \circ \mathcal{E}_{\mathbf{I}^{\otimes n_{1}} \otimes \mathbf{I}^{\otimes n_{2}} \otimes D_{3}} \right], \tag{S51}$$

where $\mathcal{E}_U(\cdot) := U \cdot U^{\dagger}$ and \mathbb{E}_{D_i} denotes the average over all operators given by Eq. (S45), (S47), and (S48). From Eq. (S44), we can decompose the symmetric Clifford twirling superchannel $\mathscr{T}_{\mathcal{Q}_U}$ as

$$\mathscr{T}_{\mathcal{O}_U}(\mathcal{E}_P) = \mathcal{E}_{W^{\dagger}} \circ (\mathscr{T}_3 * \mathscr{T}_2 * \mathscr{T}_1(\mathcal{E}_{WPW^{\dagger}})) \circ \mathcal{E}_W, \tag{S52}$$

where we define the composition of superchannels as $\mathcal{T}_2 * \mathcal{T}_1(\cdot) := \mathcal{T}_2(\mathcal{T}_1(\cdot))$. Eq. (S52) implies that it is sufficient to consider $\mathcal{T}_3 * \mathcal{T}_2 * \mathcal{T}_1(\mathcal{E}_{WPW^{\dagger}})$ in order to know $\mathcal{T}_{Q_U}(\mathcal{E}_P)$. Since W is a Clifford unitary, WPW^{\dagger} is a Pauli operator and can be decomposed as $WPW^{\dagger} = P_1 \otimes P_2 \otimes P_3$ up to phase with $P_1 \in \mathcal{P}_{n_1}$, $P_2 \in \mathcal{P}_{n_2}$, and $P_3 \in \mathcal{P}_{n_3}$ in the same way as in Eq. (S39). Below, we see how the Pauli channel $\mathcal{E}_{WPW^{\dagger}}$ is mapped by the superchannels in Eq. (S52), especially in the following four cases.

First, we consider the case where $P_2 \in \{I,Z\}^{\otimes n_2}$ and $P_3 = I^{\otimes n_3}$. Since $I^{\otimes n_1} \otimes D_1$, $I^{\otimes n_1} \otimes D_2 \otimes I^{\otimes n_3}$, and $I^{\otimes n_1} \otimes I^{\otimes n_2} \otimes D_3$ all commutes with $WPW^{\dagger} = P_1 \otimes P_2 \otimes I^{\otimes n_3}$ for $P_2 \in \{I,Z\}^{\otimes n_2}$, we can easily see that

$$\mathscr{T}_3 * \mathscr{T}_2 * \mathscr{T}_1(\mathcal{E}_{P_1 \otimes P_2 \otimes \mathbf{I} \otimes n_3}) = \mathcal{E}_{P_1 \otimes P_2 \otimes \mathbf{I} \otimes n_3}. \tag{S53}$$

Next, we consider the case where $P_2 \in \{I,Z\}^{\otimes n_2}$ and $P_3 \neq I^{\otimes n_3}$. Since $P_1 \otimes P_2 \otimes I^{\otimes n_3}$ commutes with all D_i , we only need to consider the case with $WPW^{\dagger} = I^{\otimes n_1} \otimes I^{\otimes n_2} \otimes P_3$. Since $\Lambda_i(R_i)^{\dagger} P_3 \Lambda_i(R_i) = P_3$ when $[R_i, P_3] = 0$, $\Lambda_i(R_i)^{\dagger} P_3 \Lambda_i(R_i) = Z_i P_3$ when $\{R_i, P_3\} = 0$, and Pauli operator R_i which commutes or anticommutes with P_3 appears with equal frequency under the average of D_1 , we obtain

$$\mathcal{I}_{1}(\mathcal{E}_{\mathbb{I}^{\otimes n_{1}} \otimes \mathbb{I}^{\otimes n_{2}} \otimes P_{3}}) = \mathbb{E}_{Q_{2} \in \{\mathbb{I}, \mathbb{Z}\}^{\otimes n_{2}}}[\mathcal{E}_{\mathbb{I}^{\otimes n_{1}} \otimes Q_{2} \otimes P_{3}}]. \tag{S54}$$

In addition, since D_2 represented as in Eq. (S47) commutes with Pauli-Z operator, we obtain

$$\mathcal{I}_{2}(\mathcal{E}_{\mathbb{I}^{\otimes n_{1}} \otimes Q_{2} \otimes P_{3}}) = \mathcal{E}_{\mathbb{I}^{\otimes n_{1}} \otimes Q_{2} \otimes P_{3}} \tag{S55}$$

for $Q_2 \in \{I, Z\}^{\otimes n_2}$. Furthermore, since \mathcal{T}_3 is just a Clifford twirling superchannel acting on the last n_3 qubits, we obtain

$$\mathscr{T}_3(\mathcal{E}_{\mathbf{I}^{\otimes n_1} \otimes Q_2 \otimes P_3}) = \mathbb{E}_{Q_3 \in \mathcal{P}_{n_3} \setminus \{\mathbf{I}\}^{\otimes n_3}} [\mathcal{E}_{\mathbf{I}^{\otimes n_1} \otimes Q_2 \otimes Q_3}]. \tag{S56}$$

Therefore, we have

$$\mathscr{T}_3 * \mathscr{T}_2 * \mathscr{T}_1(\mathcal{E}_{\mathbf{I} \otimes n_1 \otimes \mathbf{I} \otimes n_2 \otimes P_3}) = \mathbb{E}_{Q_2 \in \{\mathbf{I}, \mathbf{Z}\} \otimes n_2} \mathbb{E}_{Q_3 \in \mathcal{P}_{n_3} \setminus \{\mathbf{I}\} \otimes n_3} [\mathcal{E}_{\mathbf{I} \otimes n_1 \otimes Q_2 \otimes Q_3}]. \tag{S57}$$

Then, we consider the case where $P_2 \notin \{I,Z\}^{\otimes n_2}$ and $P_3 = I^{\otimes n_3}$. Since $P_1 \otimes P_{2,z} \otimes I^{\otimes n_3}$ commutes with all D_i for $P_{2,z} \in \{I,Z\}^{\otimes n_2}$, we only need to consider the case with $WPW^{\dagger} = I^{\otimes n_1} \otimes P_{2,x} \otimes I^{\otimes n_3}$ for $P_{2,x} \in \{I,X\}^{\otimes n_2} \setminus \{I\}^{\otimes n_2}$. Since $\Lambda_i(R_i)^{\dagger}X_i\Lambda_i(R_i) = X_iR_i$, where X_i being the Pauli-X operator acting on the *i*-th qubit, and all $R_i \in \mathcal{P}_{n_3}$ appears with equal frequency under the average of D_1 , we obtain

$$\mathcal{I}_{1}(\mathcal{E}_{\mathbf{I}^{\otimes n_{1}} \otimes P_{2,x} \otimes \mathbf{I}^{\otimes n_{3}}}) = \mathbb{E}_{Q_{3} \in \mathcal{P}_{n_{2}}}[\mathcal{E}_{\mathbf{I}^{\otimes n_{1}} \otimes P_{2,x} \otimes Q_{3}}]. \tag{S58}$$

In addition, since $CZ_{12}X_1CZ_{12}^{\dagger} = X_1Z_2$ and $SXS^{\dagger} = iXZ$, Pauli-X operator belonging to the middle n_2 qubit generates Pauli-Z operator with probability 1/2 for each of the n_2 qubit under the conjugation of random D_2 , and thus

$$\mathscr{T}_2(\mathcal{E}_{\mathbf{I}^{\otimes n_1} \otimes P_{2,x} \otimes Q_3}) = \mathbb{E}_{Q_2 \in \{\mathbf{I},\mathbf{Z}\}^{\otimes n_2}}[\mathcal{E}_{\mathbf{I}^{\otimes n_1} \otimes P_{2,x} Q_2 \otimes Q_3}]. \tag{S59}$$

Furthermore, since \mathcal{I}_3 is just a Clifford twirling superchannel acting on the last n_3 qubits, we obtain

$$\mathcal{I}_{3}(\mathcal{E}_{\mathbf{I}^{\otimes n_{1}} \otimes P_{2,x}Q_{2} \otimes Q_{3}}) = \mathbb{E}_{Q_{3}' \in \mathcal{P}_{n_{3}}}[\mathcal{E}_{\mathbf{I}^{\otimes n_{1}} \otimes P_{2,x}Q_{2} \otimes Q_{3}'}]. \tag{S60}$$

Therefore, we have

$$\mathscr{T}_3 * \mathscr{T}_2 * \mathscr{T}_1(\mathcal{E}_{\mathbf{I}^{\otimes n_1} \otimes P_{2x} \otimes \mathbf{I}^{\otimes n_3}}) = \mathbb{E}_{Q_2 \in \{\mathbf{I}, \mathbf{Z}\}^{\otimes n_2}} \mathbb{E}_{Q_3 \in \mathcal{P}_{n_3}} [\mathcal{E}_{\mathbf{I}^{\otimes n_1} \otimes P_{2x} Q_2 \otimes Q_3}]. \tag{S61}$$

Finally, we consider the case where $P_2 \notin \{\mathrm{I}, \mathrm{Z}\}^{\otimes n_2}$ and $P_3 \neq \mathrm{I}^{\otimes n_3}$. Since $P_1 \otimes P_{2,z} \otimes \mathrm{I}^{\otimes n_3}$ commutes with all D_i for $P_{2,z} \in \{\mathrm{I}, \mathrm{Z}\}^{\otimes n_2}$, we only need to consider the case with $WPW^\dagger = \mathrm{I}^{\otimes n_1} \otimes P_{2,x} \otimes P_3$ for $P_{2,x} \in \{\mathrm{I}, \mathrm{X}\}^{\otimes n_2} \setminus \{\mathrm{I}\}^{\otimes n_2}$. Under the conjugation of D_1 , we can see that $P = \mathrm{I}^{\otimes n_1} \otimes P_{n_2,x} \otimes P_3$ is mapped in the form of

$$(\mathbf{I}^{\otimes n_1} \otimes D_1)(\mathbf{I}^{\otimes n_1} \otimes P_{2,x} \otimes P_3)(\mathbf{I}^{\otimes n_1} \otimes D_1)^{\dagger} = \mathbf{I}^{\otimes n_1} \otimes P_{2,x}Q_2 \otimes Q_3, \tag{S62}$$

where $Q_2 \in \{I, Z\}^{\otimes n_2}$ and $Q_3 \in \mathcal{P}_{n_3}$. Here, all $Q_3 \in \mathcal{P}_{n_3}$ appears with equal probability when we randomly choose D_1 . When we think of applying $\mathscr{T}_3 * \mathscr{T}_2$ to this Pauli channel, we obtain

$$\mathcal{J}_{3} * \mathcal{J}_{2}(\mathcal{E}_{\mathbf{I}^{\otimes n_{1}} \otimes P_{2,x}Q_{2} \otimes Q_{3}}) = \begin{cases}
\mathbb{E}_{Q_{2}' \in \{\mathbf{I},\mathbf{Z}\}^{\otimes n_{2}}} \mathbb{E}_{Q_{3}' \in \mathcal{P}_{n_{3}} \setminus \{\mathbf{I}\}^{\otimes n_{3}}} [\mathcal{E}_{\mathbf{I}^{\otimes n_{1}} \otimes P_{2,x}Q_{2}' \otimes Q_{3}'}]. & (Q_{3} \neq \mathbf{I}^{\otimes n_{3}}) \\
\mathbb{E}_{Q_{2}' \in \{\mathbf{I},\mathbf{Z}\}^{\otimes n_{2}}} [\mathcal{E}_{\mathbf{I}^{\otimes n_{1}} \otimes P_{2,x}Q_{2}' \otimes \mathbf{I}^{\otimes n_{3}}}]. & (Q_{3} = \mathbf{I}^{\otimes n_{3}})
\end{cases}$$
(S63)

from the discussion of the other case. By recalling that every $Q_3 \in \mathcal{P}_{n_3}$ appears with equal probability when we randomly choose D_1 , we obtain

$$\mathcal{T}_3 * \mathcal{T}_2 * \mathcal{T}_1(\mathcal{E}_{\mathbf{I} \otimes n_1 \otimes P_{2-x} \otimes P_3}) = \mathbb{E}_{O_2 \in \{\mathbf{I}, \mathbf{Z}\} \otimes n_2} \mathbb{E}_{Q_3 \in \mathcal{P}_{n_0}} [\mathcal{E}_{\mathbf{I} \otimes n_1 \otimes P_{2-x} Q_2 \otimes Q_3}]. \tag{S64}$$

By combining Eqs. (S52), (S53), (S57), (S61), and (S64), we arrive at the conclusion of Theorem 2. \Box

S8. PROOF OF THEOREM S1

In this section, we present the proof of Theorem S1. This proof mainly follows the discussion of Sec. 5.2 of Ref. [29].

Proof. Since the n-qubit Clifford group \mathcal{G}_n is a unitary 2-design and we only consider up to a second moment in the following proof, we can assume that each Clifford gate C_l is sampled randomly from n-qubit unitary group according to the Haar measure. Since the Haar measure on the unitary group is invariant under the right and left multiplication of unitary gates, we can insert any unitary gates before and after C_l , so we can neglect the non-Clifford layer \mathcal{U} and assume that the observable O can be diagonalized using the computational basis $\{|x\rangle\}_x$ as $O = \sum_x o_x |x\rangle\langle x|$, where $-1 \le o_x \le 1$ and $\sum_x o_x = 0$. Therefore, by defining the probability distributions p_{ideal} and p_{noisy} as

$$p_{\text{ideal}}(x) = \text{tr}[|x\rangle\langle x| \mathcal{C}_{L+1} \circ \mathcal{C}_L \circ \cdots \circ \mathcal{C}_1(|0^n\rangle\langle 0^n|)], \tag{S65}$$

$$p_{\text{noisy}}(x) = \text{tr}[|x\rangle\langle x| \mathcal{C}_{L+1} \circ \mathcal{N} \circ \mathcal{C}_L \circ \cdots \circ \mathcal{N} \circ \mathcal{C}_1(|0^n\rangle\langle 0^n|)], \tag{S66}$$

we can upper-bound the average bias as

$$\mathbb{E}_{C}[|R\mathrm{tr}[\rho_{\mathrm{noisy}}O] - \mathrm{tr}[\rho_{\mathrm{ideal}}O]|] = \mathbb{E}_{C}\left[\left|\sum_{x} o_{x} \left(Rp_{\mathrm{noisy}}(x) + (1-R)2^{-n} - p_{\mathrm{ideal}}(x)\right)\right|\right]$$
(S67)

$$\leq \mathbb{E}_C \left[\sum_{x} \left| \left(R p_{\text{noisy}}(x) + (1 - R) 2^{-n} - p_{\text{ideal}}(x) \right) \right| \right]$$
 (S68)

$$\leq \mathbb{E}_C \left[2^{n/2} \sqrt{\sum_{x} (Rp_{\text{noisy}}(x) + (1-R)2^{-n} - p_{\text{ideal}}(x))^2} \right]$$
 (S69)

$$\leq \sqrt{2^n \mathbb{E}_C \left[\sum_{x} (Rp_{\text{noisy}}(x) + (1-R)2^{-n} - p_{\text{ideal}}(x))^2 \right]}, \tag{S70}$$

where we used $\sum_x o_x = 0$ in the first equality, the triangle inequality and $|o_x| \le 1$ in the second inequality, $\|\mathbf{v}\|_1 \le 2^{n/2} \|\mathbf{v}\|_2$ for 2^n -dimensional vector \mathbf{v} in the third inequality, and Jensen's inequality in the last inequality. Then, by defining

$$Z_0 = 2^n \mathbb{E}_C \left[\sum_x p_{\text{ideal}}(x)^2 \right]$$
 (S71)

$$= 2^{2n} \mathbb{E}_C \left[p_{\text{ideal}}(0^n)^2 \right], \tag{S72}$$

$$Z_1 = 2^n \mathbb{E}_C \left[\sum_x p_{\text{ideal}}(x) p_{\text{noisy}}(0^n) \right]$$
 (S73)

$$= 2^{2n} \mathbb{E}_C[p_{\text{ideal}}(0^n) p_{\text{noisy}}(0^n)], \tag{S74}$$

$$Z_2 = 2^n \mathbb{E}_C \left[\sum_x p_{\text{noisy}}(x)^2 \right]$$
 (S75)

$$= 2^{2n} \mathbb{E}_C \left[p_{\text{noisy}}(0^n)^2 \right], \tag{S76}$$

we obtain

$$\mathbb{E}_{C}[|R\text{tr}[\rho_{\text{noisy}}O] - \text{tr}[\rho_{\text{ideal}}O]|] \leq \sqrt{2^{n}\mathbb{E}_{C}\left[\sum_{x}(R(p_{\text{noisy}}(x) - 2^{-n}) - (p_{\text{ideal}}(x) - 2^{-n}))^{2}\right]}$$

$$= \sqrt{R^{2}(Z_{2} - 1) - 2R(Z_{1} - 1) + (Z_{0} - 1)},$$
(S78)

where the RHS is minimized when we take $R = \frac{Z_1 - 1}{Z_2 - 1}$. In this case, we obtain

$$\mathbb{E}_{C}[|R\mathrm{tr}[\rho_{\mathrm{noisy}}O] - \mathrm{tr}[\rho_{\mathrm{ideal}}O]|] \le \sqrt{(Z_0 - 1)\left(1 - \frac{(Z_1 - 1)^2}{(Z_2 - 1)(Z_0 - 1)}\right)}.$$
 (S79)

Now, let us analyze Z_0 , Z_1 , and Z_2 . By using the 2-moment operator defined in Eq. (S22), we obtain

$$Z_0 = 2^{2n} \mathbb{E}_C \left[\operatorname{tr} \left[|0^n\rangle \langle 0^n| \, \mathcal{C}_{L+1} \circ \mathcal{C}_L \circ \cdots \circ \mathcal{C}_1 (|0^n\rangle \langle 0^n|) \right]^2 \right]$$
 (S80)

$$= 2^{2n} \mathbb{E}_{C} \left[\operatorname{tr}[(|0^{n}\rangle\langle 0^{n}| \mathcal{C}_{L+1} \circ \mathcal{C}_{L} \circ \cdots \circ \mathcal{C}_{1}(|0^{n}\rangle\langle 0^{n}|))^{\otimes 2}] \right]$$
 (S81)

$$= 2^{2n} \mathbb{E}_{C} \left[\operatorname{tr} \left[|0^{2n} \rangle \langle 0^{2n} | \mathcal{C}_{L+1}^{\otimes 2} \circ \mathcal{C}_{L}^{\otimes 2} \circ \cdots \circ \mathcal{C}_{1}^{\otimes 2} (|0^{2n} \rangle \langle 0^{2n} |) \right] \right]$$
(S82)

$$= 2^{2n} \operatorname{tr}[|0^{2n}\rangle\langle 0^{2n}| \underbrace{\mathcal{M} \circ \cdots \circ \mathcal{M}}_{L+1}(|0^{2n}\rangle\langle 0^{2n}|)]]. \tag{S83}$$

In the same way, we obtain

$$Z_{i} = 2^{2n} \operatorname{tr}[|0^{2n}\rangle\langle 0^{2n}| \underbrace{\mathcal{M} \circ \mathcal{N}_{i} \circ \cdots \circ \mathcal{M} \circ \mathcal{N}_{i}}_{L} \circ \mathcal{M}(|0^{2n}\rangle\langle 0^{2n}|)]]$$
(S84)

for i = 0, 1, 2, where we have defined

$$\mathcal{N}_0 = \mathcal{I} \otimes \mathcal{I}, \tag{S85}$$

$$\mathcal{N}_1 = \mathcal{I} \otimes \mathcal{N}, \tag{S86}$$

$$\mathcal{N}_2 = \mathcal{N} \otimes \mathcal{N} \tag{S87}$$

using the identity channel \mathcal{I} .

We next analyze Eq. (S84). From Eq. (S22), we have

$$\mathcal{M}(|0^{2n}\rangle\langle 0^{2n}|) = \left(1 - \frac{1}{2^n + 1}\right) \frac{\mathbb{I}}{2^{2n}} + \frac{1}{2^n + 1} \frac{\mathbb{F}}{2^n}.$$
 (S88)

Next, we calculate the action of $\mathcal{M} \circ \mathcal{N}_i$ on $\mathbb{I}/2^{2n}$ and $\mathbb{F}/2^n$. Since \mathcal{I} and \mathcal{N} are both unital, we obtain

$$\mathcal{M} \circ \mathcal{N}_i \left(\frac{\mathbb{I}}{2^{2n}} \right) = \frac{\mathbb{I}}{2^{2n}} \tag{S89}$$

for i = 0, 1, 2. For the input state $\mathbb{F}/2^n$, we obtain

$$\mathcal{M} \circ \mathcal{N}_0 \left(\frac{\mathbb{F}}{2^n} \right) = \mathcal{M} \left(\frac{\mathbb{F}}{2^n} \right)$$
 (S90)

$$= \frac{\mathbb{F}}{2^n},\tag{S91}$$

$$= \frac{\mathbb{F}}{2^n},$$

$$\mathcal{M} \circ \mathcal{N}_1 \left(\frac{\mathbb{F}}{2^n} \right) = 2^{-n} \mathcal{M}(\mathcal{I} \otimes \mathcal{N}(\mathbb{F}))$$
(S92)

$$= \frac{2^{n} \operatorname{tr}[\mathcal{I} \otimes \mathcal{N}(\mathbb{F})] - \operatorname{tr}[\mathcal{I} \otimes \mathcal{N}(\mathbb{F})\mathbb{F}]}{2^{2n} - 1} \frac{\mathbb{I}}{2^{2n}} + \frac{\operatorname{tr}[\mathcal{I} \otimes \mathcal{N}(\mathbb{F})\mathbb{F}] - 2^{-n} \operatorname{tr}[\mathcal{I} \otimes \mathcal{N}(\mathbb{F})]}{2^{2n} - 1} \frac{\mathbb{F}}{2^{n}}$$
(S93)

$$= (1-s)\frac{\mathbb{I}}{2^{2n}} + s\frac{\mathbb{F}}{2^{2n}},\tag{S94}$$

$$\mathcal{M} \circ \mathcal{N}_2\left(\frac{\mathbb{F}}{2^n}\right) = 2^{-n}\mathcal{M}(\mathcal{N} \otimes \mathcal{N}(\mathbb{F}))$$
 (S95)

$$= \frac{2^{n} \operatorname{tr}[\mathcal{N} \otimes \mathcal{N}(\mathbb{F})] - \operatorname{tr}[\mathcal{N} \otimes \mathcal{N}(\mathbb{F})\mathbb{F}]}{2^{2n} - 1} \frac{\mathbb{I}}{2^{2n}} + \frac{\operatorname{tr}[\mathcal{N} \otimes \mathcal{N}(\mathbb{F})\mathbb{F}] - 2^{-n} \operatorname{tr}[\mathcal{N} \otimes \mathcal{N}(\mathbb{F})]}{2^{2n} - 1} \frac{\mathbb{F}}{2^{n}}$$
(S96)

$$= (1 - u)\frac{\mathbb{I}}{2^{2n}} + u\frac{\mathbb{F}}{2^{2n}},\tag{S97}$$

where we have used

$$\operatorname{tr}[\mathcal{I} \otimes \mathcal{N}(\mathbb{F})] = \sum_{i} \operatorname{tr}[(I \otimes E_{i})\mathbb{F}(I \otimes E_{i}^{\dagger})]$$
 (S98)

$$= \sum_{i} \operatorname{tr}[E_{i}E_{i}^{\dagger}] \tag{S99}$$

$$= 2^n, (S100)$$

$$= 2 ,$$

$$\operatorname{tr}[\mathcal{I} \otimes \mathcal{N}(\mathbb{F})\mathbb{F}] = \sum_{i} \operatorname{tr}[(I \otimes E_{i})\mathbb{F}(I \otimes E_{i}^{\dagger})\mathbb{F}]$$
(S100)

$$= \sum_{i} \operatorname{tr}[E_{i}] \operatorname{tr}[E_{i}^{\dagger}] \tag{S102}$$

$$= (2^{2n} - 1)s + 1, (S103)$$

$$= (2^{2n} - 1)s + 1,$$

$$\operatorname{tr}[\mathcal{N} \otimes \mathcal{N}(\mathbb{F})] = \sum_{ij} \operatorname{tr}[(E_j \otimes E_i)\mathbb{F}(E_j^{\dagger} \otimes E_i^{\dagger})]$$
(S103)

$$= \sum_{ij} \operatorname{tr}[E_i E_j^{\dagger} E_j E_i^{\dagger}] \tag{S105}$$

$$= 2^n, (S106)$$

$$= 2^{n},$$

$$\operatorname{tr}[\mathcal{N} \otimes \mathcal{N}(\mathbb{F})\mathbb{F}] = \sum_{i} \operatorname{tr}[(E_{j} \otimes E_{i})\mathbb{F}(E_{j} \otimes E_{i}^{\dagger})\mathbb{F}]$$
(S106)
$$(S107)$$

$$= \sum_{i} \operatorname{tr}[E_{i}E_{j}^{\dagger}]\operatorname{tr}[E_{i}^{\dagger}E_{j}]$$
 (S108)

$$= (2^{2n} - 1)u + 1. (S109)$$

Therefore, we obtain

$$Z_0 = 2^{2n} \left(\left(1 - \frac{1}{2^n + 1} \right) \frac{\operatorname{tr}[|0^{2n} \rangle \langle 0^{2n} | \mathbb{I}]}{2^{2n}} + \frac{1}{2^n + 1} \frac{\operatorname{tr}[|0^{2n} \rangle \langle 0^{2n} | \mathbb{F}]}{2^n} \right)$$
 (S110)

$$= 1 + \frac{2^n - 1}{2^n + 1},\tag{S111}$$

$$Z_{1} = 2^{2n} \left(\left(1 - \frac{1}{2^{n} + 1} s^{L} \right) \frac{\operatorname{tr}[|0^{2n} \rangle \langle 0^{2n} | \mathbb{I}]}{2^{2n}} + \frac{1}{2^{n} + 1} s^{L} \frac{\operatorname{tr}[|0^{2n} \rangle \langle 0^{2n} | \mathbb{F}]}{2^{n}} \right)$$
 (S112)

$$= 1 + \frac{2^n - 1}{2^n + 1} s^L, \tag{S113}$$

$$Z_{2} = 2^{2n} \left(\left(1 - \frac{1}{2^{n} + 1} u^{L} \right) \frac{\operatorname{tr}[|0^{2n}\rangle\langle 0^{2n}|\mathbb{I}]}{2^{2n}} + \frac{1}{2^{n} + 1} u^{L} \frac{\operatorname{tr}[|0^{2n}\rangle\langle 0^{2n}|\mathbb{F}]}{2^{n}} \right)$$
(S114)

$$= 1 + \frac{2^n - 1}{2^n + 1} u^L. \tag{S115}$$

Thus, we have

$$\mathbb{E}_{C}[|R\mathrm{tr}[\rho_{\mathrm{noisy}}O] - \mathrm{tr}[\rho_{\mathrm{ideal}}O]|] \leq \sqrt{\frac{2^{n} - 1}{2^{n} + 1} \left(1 - \left(\frac{s^{2}}{u}\right)^{L}\right)}.$$
 (S116)

for
$$R = (s/u)^L$$
.

For Pauli noise $\mathcal{N} = (1 - p_{\text{err}})\mathcal{I} + \sum_{i} p_{i} \mathcal{E}_{P_{i}}$, we can calculate the RHS of Eq. (S116) as

$$\sqrt{\frac{2^{n}-1}{2^{n}+1}\left(1-\left(\frac{s^{2}}{u}\right)^{L}\right)} = \sqrt{\frac{2^{n}-1}{2^{n}+1}\left(1-\left(1-\frac{4^{n}}{4^{n}-1}\left(\sum_{i}p_{i}^{2}-\frac{1}{4^{n}-1}p_{\mathrm{err}}^{2}\right)+O(p_{i}^{3})\right)^{L}}\right)$$
(S117)

$$= \sqrt{\frac{2^n - 1}{2^n + 1} \left(1 - \left(1 - \frac{4^n}{4^n - 1} v^2 p_{\text{err}}^2 + O(p_i^3) \right)^L \right)}$$
 (S118)

where we use Eq. (S31) and (S32). Especially when we assume that $p_{\rm tot}=p_{\rm err}L$ is constant and $L\gg 1$, we have

$$\sqrt{\frac{2^{n}-1}{2^{n}+1}\left(1-\left(\frac{s^{2}}{u}\right)^{L}\right)} \sim \sqrt{\frac{2^{n}-1}{2^{n}+1}\left(1-\left(1-\frac{4^{n}}{4^{n}-1}\frac{v^{2}p_{\text{tot}}^{2}}{L^{2}}\right)^{L}\right)}$$
(S119)

$$\sim \sqrt{\frac{2^{n}-1}{2^{n}+1} \frac{4^{n}}{4^{n}-1} \frac{v^{2} p_{\text{tot}}^{2}}{L}}$$

$$\leq \frac{v p_{\text{tot}}}{\sqrt{L}}$$
(S120)

$$\leq \frac{vp_{\text{tot}}}{\sqrt{L}}$$
(S121)

up to the leading order of L. Therefore, we obtain Corollary S1.